Biochemical Pharmacology 82 (2011) 755–768

Contents lists available at ScienceDirect

Biochemical Pharmacology

journal homepage: www.elsevier.com/locate/biochempharm

Discovery of a novel COX-2 inhibitor as an orally potent anti-pyretic and anti-inflammatory drug: Design, synthesis, and structure–activity relationship

Shigeo Hayashi *, Yoko Sumi, Naomi Ueno, Akio Murase, Junji Takada

Pfizer Global Research & Development, Nagoya Laboratories, Pfizer Japan Inc., 5-2 Taketoyo, Aichi 470-2393, Japan

ARTICLE INFO

Article history:
Received 28 March 2011
Accepted 23 June 2011
Available online 2 July 2011

Keywords:
NSAID
COX-2/COX-1 selectivity
Orally active COX-2 inhibitor
LPS-induced fever
Carrageenan-induced edema
Inflammation

ABSTRACT

Cyclooxygenase (COX) has been considered as a significant pharmacological target because of its pivotal roles in the prostaglandin biosynthesis and following cascades that lead to various (patho)physiological effects. Non-steroidal anti-inflammatory drugs (NSAIDs) that suppress COX activities have been used clinically for the treatment of fever, inflammation, and pain; however, nonselective COX inhibitors exhibit serious side-effects such as gastrointestinal damage because of their inhibitory activities against COX-1. Thus, COX-1 is constitutive and expressed ubiquitously and serves a housekeeping role, while COX-2 is inducible or upregulated by inflammatory/injury stimuli such as interleukin-1β, tumor necrosis factor-α, and lipopolysaccharide in macrophage, monocyte, synovial, liver, and lung, and is associated with prostaglandin E_2 and prostacyclin production that evokes or sustains systemic/peripheral inflammatory symptoms. Also, hypersensitivity of aspirin is a significant concern clinically. Hence, design, synthesis, and structure–activity relationship of [2-{[(4-substituted)-pyridin-2-yl]carbonyl}-(6- or 5-substituted)-1*H*-indol-3-yl]acetic acid analogues were investigated to discover novel acid-type COX-2 inhibitor as an orally potent new-class anti-pyretic and anti-inflammatory drug. As significant findings, compounds **1**–**3** demonstrated potent COX-2 inhibitory activities with high selectivities for COX-2 over COX-1 in human cells or whole-blood *in vitro*, and demonstrated orally potent anti-pyretic activity against lipopolysaccharide-induced systemic-inflammatory fever model in F344 rats. Also compound **1** demonstrated orally potent anti-inflammatory activity against edema formation and a suppressive effect against PGE_2 production in carrageenan-induced peripheral-inflammation model on the paw of SD rats. These results suggest that compounds **1**–**3** are potential agents for the treatment of inflammatory disease and are useful for further pharmacological COX-2 inhibitor investigations.

1. Introduction

In the human body the arachidonic acid (AA), that is released from phospholipids of cellular membrane by phospholipase A_2 (PLA_2) mediated-hydrolysis [1], is converted into prostaglandin (PG) H_2 (PGH_2) catalyzed by cyclooxygenase (COX, or prostaglandin G/H synthase or endoperoxidase; EC 1.14.99.1) [2–4] by way of the addition of two O_2 (oxygen) molecules onto AA to form PGG_2 followed by the reduction of the hydroperoxide group of PGG_2 to form PGH_2 using two distinctive catalytic sites, the cyclooxygenase and peroxidase sites in the COX protein [5,6]. Furthermore, PGH_2 is metabolized into various types of prostanoids (eicosanoids), namely, PGs such as PGE_2, PGD_2, and $PGF_{2\alpha}$, prostacyclin (PGI_2), and thromboxane (TX) A_2 (TXA_2) that is rapidly converted into TXB_2 [1,5]. These prostanoids bind with respective specific G-protein-coupled-receptors (GPCRs), and play various types of key roles for regulation of human physiology and pathophysiology; for example, PGE_2 closely associates with inflammation, fever, and pain, and PGI_2 closely associates with inflammation, pain, and vasodilation. Particularly in the inflammatory process, PGE_2 and PGI_2 play critical roles to cause increases in body temperature, vascular permeability, and edema as inflammatory-disease mediators [1,5,7–10]. Since COX is a key rate-limiting enzyme for PG production, and inhibition of COX activity is able to attenuate the levels of PGs that are involved in the inflammatory symptoms such as heat, swelling, flare, and pain, COX inhibition has been

Abbreviations: COX, cyclooxygenase (or endoperoxidase, or prostaglandin G/H synthase, EC 1.14.99.1); AA, arachidonic acid; PG, prostaglandin; PGH_2, prostaglandin H_2; PGG_2, prostaglandin G_2; PGE_2, prostaglandin E_2; PGI_2, prostacyclin; 6-keto-$PGF_{1\alpha}$, 6-keto-prostaglandin $F_1\alpha$; TXA_2, thromboxane A_2; TXB_2, thromboxane B_2; NSAID, non-steroidal anti-inflammatory drug; SPF, specific pathogen free; VAF, virus antibody free; F344 rat, Fischer 344 rat; SD rat, Sprague–Dawley rat; TNF-α, tumor necrosis factor-α; IL-1β, interleukin-1β; IL-6β, interleukin-6β; DBU, 1,8-diazabicyclo[5.4.0]undec-7-ene; LPS, lipopolysaccharide; HUVEC, human umbilical vein endothelial cell; HWP, human washed platelet; RA, rheumatoid arthritis; OA, osteoarthritis; HBD, hydrogen bond donor; HBA, hydrogen bond acceptor.

* Corresponding author.
E-mail address: Shigeo_Hayashi@nifty.com (S. Hayashi).

0006-2952/$ – see front matter © 2011 Elsevier Inc. All rights reserved.
doi:10.1016/j.bcp.2011.06.036

Table 1
Induction or overexpression of COX-2 in the various types of organs, tissues, and cells in the reported studies.

Induction or overexpression site	Condition[a]	Reference[b]
Liver or hepatocytes	A and B	[13,14,26]
Lung	A	[13,14]
Macrophages	A, B, C, and D	[11,25–27]
Monocytes	A, B, D, and E	[3,11,25,26,28]
Bloods	A and B	[3,26]
Perivascular areas and lymphoid aggregates	D	[11]
Endothelial cells	C, D, and E	[11,27,28]
Vascular smooth muscle cells	F	[29]
Synovial tissues, synoviocytes or joint	D, G, H, and I	[11,30,31]
Paw	J	[23]
Cartilage	K	[32]
Articular chondrocytes	L	[33]
Neutrophils	M	[34]
Peripheral nerves	N	[35]
Spinal cord	C, O, and P	[23,27,36]
Fibroblasts	B and Q	[26,37]
Precancer lesions or tumor cells	R and S	[38,39]
Surgical peripheral tissues	T	[40]

[a] A: bacterial lipopolysaccharide (LPS) [3,13,14,25]; B: virus(es) [26]; C: interleukin-1β (IL-1β) [27]; D: human rheumatoid arthritis (RA) [11]; E: LPS or phorbol 12-myristate 13-acetate (PMA, a tumor promoter) [28]; F: IL-1β or a mixture of IL-1β, tumor necrosis factor-α (TNF-α), interferon-γ (IFN-γ), and LPS [29]; G: rat adjuvant-induced arthritis [11]; H: human ankylosing spondylitis (AS), human psoriatic arthritis (PsA) or human RA [30]; I: activated T lymphocytes, IL-1β, IL-17 or TNF-α [31]; J: rat adjuvant-induced edema [23]; K: human osteoarthritis (OA) [32]; L: IL-1β TNF-α, IL-6, leukemia inhibitory factor (LIF) or LPS [33]; M: LPS, TNF-α, granulocyte-macrophage colony-stimulating factor (GM-CSF) or PMA [34]; N: human classic Guillain–Barré syndrome (GBS), human chronic inflammatory demyelinating polyradiculoneuropathy (CIDP) or human vasculitic neuropathy (VN) [35]; O: local adjuvant-injection in rats [23]; P: local carrageenan-injection in rats [36]; Q: LPS, IL-1β, TNF-α or PMA [37]; R: epidermal growth factor receptor (EFGR) or type-α transforming growth factor (TGF-α) [38]; S: IL-1β or IL-1β-induced activation of nuclear factor κB (NF-κB) and p38 [39]; T: oral surgery in human [40].

[b] Reference number cited in the text.

considered as a significant target of drug candidates for the treatment of pyrexia, inflammation, and pain [5].

Historically, non-steroidal anti-inflammatory drugs (NSAIDs), for example, aspirin (acetylsalicylic acid), indomethacin, ibuprofen, and naproxen, have been used clinically for the treatment of pyrexia, inflammation that includes rheumatoid arthritis (RA) and osteoarthritis (OA), and pain, by virtue of their suppression of the effects on COX activity [1,5,7,9,11–18]; however, these agents have exhibited side-effect issues such as gastrointestinal (GI) tract bleeding, ulcer, and perforation [19–21]. The detailed mechanisms of both the anti-inflammation effects and the side-effects are associated with the existence of two COX isoforms, namely, COX-1 (EC 1.14.99.1) and COX-2 (EC 1.14.99.1). Thus, (i) COX-1 is predominantly expressed ubiquitously and constitutively, and it serves a housekeeping role in processes such as GI mucosa protection; whereas inhibition of COX-1 activity causes GI tract damage. By contrast, (ii) COX-2 is absent or exhibits a low level of expression in most tissues, but it is constitutively expressed in some tissues such as spinal cord and dorsal root ganglions (DRGs) [22], and is inducible and upregulated by inflammatory processes [3,5,9,13,23,24] related to bacterial or viral infection, or specifically, inflammatory or tissue-injury stimuli/signals such as interleukin-1β (IL-1β), IL-6, IL-17, tumor necrosis factor-α (TNF-α), bacterial lipopolysaccharide (LPS) [3,13,14,25], viruses [26], activated T lymphocytes, and growth factors. Actually, COX-2 induction or overexpression occurs in the various types of organs, tissues, and cells [3,11,13,14,23,25–40] as summarized in Table 1. COX-2 contribution to PGE_2 and PGI_2 production evokes and sustains systemic or peripheral inflammatory disease but it is not involved in the COX-1-mediated GI tract events [19–21]. Indeed, the major issues of the nonselective COX inhibitors (as well as COX-1 selective inhibitors) in the gastrointestinal tract are due to their COX-1 inhibitory activities [19–21,41]. Significant clinical concerns due to upregulation of COX-2 under inflammatory conditions result from stimulation or increases in pro-mitogenic factors, carcinogenesis, tumor angiogenesis, and lymphangiogenesis by COX-2-derived mediators including PGs and growth factors and/or by DNA oxidative damage resulting from COX-2 activity [37–39,42–44]. Therefore, the suppressive and preventive effects on various types of cancers or tumors such as colon, lung, gastric, and intestinal cancers by inhibition of COX-2 activity have been widely studied [37,42–48]. On the other hand, it has been reported that COX-2 selective inhibition improves vascular endothelial function and reduces oxidative stress in coronary artery disease, and attenuates LPS-induced cardiovascular failure or liver injury [49,50]; although rofecoxib, a potent and selective COX-2 inhibitor, had cardiovascular risk possibly due to its structural issue [51], also it was reported that some traditional NSAIDs and COX-2 inhibitors showed respective agent-dependent potential cardiovascular risk in long-term study with attention to permanent blockade against COX-2 activity [52]. In addition, the inhibitory actions of aspirin or of some other NSAIDs against COX-1 can be crucial problems in clinical pharmacotherapy [53]. Taken together, highly selective COX-2 inhibitors have been needed for the treatment of inflammatory diseases because of safety issues related to potential COX-1 inhibition [11,41,54].

The aim of the present study is to investigate and identify an orally active novel COX-2 selective inhibitor as a new-class antipyretic and anti-inflammatory drug, with drug design and synthesis around [2-{[(4-substituted)-pyridin-2-yl]carbonyl}-(6- or 5-substituted)-1*H*-indol-3-yl]acetic acid analogues. The significant findings of novel acid-type COX-2 inhibitors are reported herein.

2. Materials and methods

2.1. Synthesis

2.1.1. General

In general, reagents, solvents, and other chemicals were used as purchased without further purification. All reactions with air- or moisture-sensitive reactants and solvents were carried out under nitrogen atmosphere unless noted otherwise. Flash column chromatography (medium pressure liquid chromatography) purifications were carried out using Merck silica gel 60 (230–400 mesh ASTM) (Merck KGaA, Darmstadt, Germany). The structures of all isolated compounds were ensured by NMR, IR, MS or elementary analysis. ^{1}H nuclear magnetic resonance (^{1}H NMR) data were determined at 270 MHz on a JNM-LA 270 (JEOL Ltd., Akishima, Tokyo, Japan) spectrometer. Chemical shifts are expressed in δ (ppm). ^{1}H NMR chemical shifts were determined relative to tetramethylsilane (TMS) as internal standard. NMR data are reported as follows: chemical shift, number of atoms, multiplicities (s, singlet; d, doublet; t, triplet; q, quartet; m, multiplet; dd, double doublet; br, broadened), and coupling constants. Infrared spectra were measured by an IR-470 (Shimadzu Co., Kyoto, Japan) infrared spectrometer. Low-resolution mass spectral data (EI) were obtained on an Automass 120 (JEOL Ltd., Akishima, Tokyo, Japan) mass spectrometer. Melting points were obtained using an Exstar 6000 (Seiko Instruments Inc., Chiba, Japan) and were uncorrected. All final compounds **1**–**3** and synthetic intermediates were synthesized by us at Pfizer Global Research & Development, Nagoya Laboratories (Aichi, Japan). The suppliers and their locations for general reagents and solvents including dry or anhydrous solvents used in this study are shown

in the following subsections, respectively. Other general reagents and solvents were purchased from Wako Pure Chemical Industries (Osaka, Japan) unless stated otherwise. All general chemicals were the highest available grade.

2.1.2. Synthesis of {2-[(4-ethylpyridin-2-yl)carbonyl]-5-(trifluoromethyl)-1H-indol-3-yl}acetic acid **1**

*2.1.2.1. Methyl (2E)-3-[2-amino-5-(trifluoromethyl)phenyl]acrylate (**5**).* A mixture of 2-bromo-4-(trifluoromethyl)aniline **4** (Avocado Research Chemicals, Lancashire, United Kingdom, 20.00 g, 83.33 mmol), methyl acrylate (Tokyo Chemical Industry, Tokyo, Japan, 18.8 mL, 209 mmol), $Pd(OAc)_2$ (Wako Pure Chemical Industries, Osaka, Japan, 2.20 g, 9.80 mmol), tri(*o*-tolyl)phosphine (Tokyo Chemical Industry, Tokyo, Japan, 12.10 g, 39.8 mmol), and dry Et_3N (Wako Pure Chemical Industries, Osaka, Japan, 45.0 mL, 323 mmol) in dry CH_3CN (Dojindo Laboratories, Kumamoto, Japan, 170 mL) was stirred under reflux conditions under N_2 for 1.5 h, then more methyl acrylate (9.40 mL, 104 mmol), $Pd(OAc)_2$ (1.10 g, 4.90 mmol), tri(*o*-tolyl)phosphine (6.10 g, 20.0 mmol), and dry Et_3N (23.0 mL, 165 mmol) were added to the mixture. The reaction mixture was further stirred under reflux conditions for 5 h, then concentrated *in vacuo*. The residue was diluted with AcOEt, washed with water, dried over anhydrous $MgSO_4$ (Wako Pure Chemical Industries, Osaka, Japan), filtered, and concentrated *in vacuo*. The residue was purified by flash column chromatography (silica gel, hexane/AcOEt = 5:1 to 2:1) to afford 14.70 g of the title product **5** in 72% yield as yellow solid. ^{1}H NMR ($CDCl_3$, 270 MHz) δ 7.76 (1H, d, J = 15.8 Hz), 7.60 (1H, m), 7.41–7.37 (1H, m), 6.74 (1H, d, J = 8.56 Hz), 6.41 (1H, d, J = 15.8 Hz), 4.27 (2H, br s), 3.82 (3H, s).

*2.1.2.2. Methyl (2E)-3-{2-[(phenylsulfonyl)amino]-5-(trifluoromethyl)phenyl}acrylate (**6**).* To a stirred solution of methyl (2*E*)-3-[2-amino-5-(trifluoromethyl)phenyl]acrylate **5** (14.70 g, 59.95 mmol) and dry pyridine (Wako Pure Chemical Industries, Osaka, Japan, 14.5 mL, 179.3 mmol) in dry CH_2Cl_2 (Wako Pure Chemical Industries, Osaka, Japan, 150 mL) was added dropwise benzenesulfonyl chloride (Tokyo Chemical Industry, Tokyo, Japan, 8.40 mL, 65.8 mmol) at room temperature under N_2. The reaction mixture was stirred at room temperature under N_2 for 9 h, allowed to stand overnight. More benzenesulfonyl chloride (1.50 mL, 11.8 mmol) was added dropwise to the mixture, and the mixture was stirred at room temperature for 3 h, then MeOH (20 mL) was added. The mixture was concentrated *in vacuo*, and the residue was diluted with AcOEt at room temperature, washed with 2 N HCl followed by washing with saturated aqueous $NaHCO_3$, dried over anhydrous $MgSO_4$, filtered, and concentrated *in vacuo*. The residue was recrystallized from dry EtOH (Wako Pure Chemical Industries, Osaka, Japan) to afford 15.12 g of the title product **6** in 65% yield as a white solid. ^{1}H NMR ($CDCl_3$, 270 MHz) δ 7.79–7.75 (2H, m), 7.66–7.54 (5H, m), 7.50–7.44 (2H, m), 7.18 (1H, br s), 6.26 (1H, d, J = 15.8 Hz), 3.81 (3H, s).

*2.1.2.3. 2-Bromo-1-(4-ethylpyridin-2-yl)ethanone (**8**).* To a solution of 2-acetyl-4-ethylpyridine **7** (synthesized at Pfizer Global Research & Development, Aichi, Japan, according to the reported procedure [55,56], 5.968 g, 40.0 mmol) in 25% HBr/AcOH (Wako Pure Chemical Industries, Osaka, Japan, 82.0 mL) was added dropwise bromine (Wako Pure Chemical Industries, Osaka, Japan, 2.27 mL, 44.3 mmol) in glacial AcOH (Wako Pure Chemical Industries, Osaka, Japan, 18.0 mL) at 0 °C under N_2 over 30 min. The reaction solution was warmed to room temperature and stirred under N_2 for 2.5 h. After some volume of the resulting mixture was reduced *in vacuo*, the mixture was diluted with anhydrous Et_2O (Wako Pure Chemical Industries, Osaka, Japan, 150 mL), cooled to 0 °C, and basified by adding saturated aqueous $NaHCO_3$ at 0 °C. The etheral layer was separated, and the aqueous layer was extracted with Et_2O (150 mL × 2). The etheral layers were combined, dried over anhydrous $MgSO_4$, filtered, then concentrated *in vacuo* to afford 10.96 g of the title product **8** as a dark-brown oil (crude). ^{1}H NMR ($CDCl_3$, 270 MHz) δ 8.56 (1H, d, J = 4.94 Hz), 7.95–7.94 (1H, m), 7.37–7.34 (1H, m), 4.86 (2H, s), 2.74 (2H, q, J = 7.56 Hz), 1.29 (3H, t, J = 7.56 Hz).

*2.1.2.4. Methyl {2-[(4-ethylpyridin-2-yl)carbonyl]-5-(trifluoromethyl)-1H-indol-3-yl}acetate (**9**).* A mixture of methyl (2*E*)-3-{2-[(phenylsulfonyl)amino]-5-(trifluoromethyl)phenyl}acrylate **6** (5.36 g, 16.0 mmol), 2-bromo-1-(4-ethylpyridin-2-yl)ethanone **8** (10.96 g, crude), and anhydrous K_2CO_3 (Wako Pure Chemical Industries, Osaka, Japan, 22.11 g, 160.0 mmol) in dry acetone (Wako Pure Chemical Industries, Osaka, Japan, 200 mL) was stirred at room temperature under N_2 for 23 h, then 1,8-diazabicyclo[5.4.0]undec-7-ene (DBU) (Wako Pure Chemical Industries, Osaka, Japan, 12.18 g, 80.0 mmol) was added. The reaction mixture was stirred at room temperature under N_2 for 12 h then concentrated *in vacuo*. The residue was purified by flash column chromatography (silica gel, hexane/AcOEt = 3:1) to afford 2.114 g of the title product **9** in 34% yield as a lemon yellow solid. ^{1}H NMR ($CDCl_3$, 270 MHz) δ 12.63 (1H, br s), 8.54 (1H, d, J = 4.94 Hz), 8.11 (1H, s), 7.94 (1H, s), 7.53–7.46 (2H, m), 7.33–7.30 (1H, m), 4.30 (2H, s), 3.77 (3H, s), 2.72 (2H, q, J = 7.59 Hz), 1.28 (3H, t, J = 7.72 Hz).

*2.1.2.5. {2-[(4-Ethylpyridin-2-yl)carbonyl]-5-(trifluoromethyl)-1H-indol-3-yl}acetic acid (**1**).* A stirred mixture of methyl {2-[(4-ethylpyridin-2-yl)carbonyl]-5-(trifluoromethyl)-1*H*-indol-3-yl}acetate **9** (2.114 g, 5.42 mmol) and 2 N NaOH (Wako Pure Chemical Industries, Osaka, Japan, 8.2 mL, 16.4 mmol) in EtOH (Wako Pure Chemical Industries, Osaka, Japan, 106.0 mL) was warmed under reflux conditions using an oil bath (~100 °C) under N_2 then turned into brown solution. The reaction solution was stirred at the same condition under N_2 for 1.5 h, cooled to room temperature, then 2 N HCl (Wako Pure Chemical Industries, Osaka, Japan, 8.2 mL) was added. The mixture was concentrated *in vacuo*, and the residue was dissolved in anhydrous THF (Dojindo Laboratories, Kumamoto, Japan), dried over anhydrous $MgSO_4$, filtered, then concentrated *in vacuo*. The residual solid was washed with AcOEt, dried under vacuum at 40 °C to afford 1.631 g of the title product **1** in 80% yield as yellow solid. Mp: 202.6 °C. ^{1}H NMR (DMSO-d_6, 270 MHz) δ 12.53 (1H, s), 8.74 (1H, d, J = 4.94 Hz), 8.24 (1H, s), 8.00 (1H, m), 7.86 (1H, d, J = 8.72 Hz), 7.64–7.58 (2H, m), 4.17 (2H, s), 2.79 (2H, q, J = 7.59 Hz), 1.26 (3H, t, J = 7.59 Hz). IR (KBr): 3275, 1705, 1647, 1597, 1537, 1448, 1339, 1279, 1204, 1163, 1051, 1024, 810, 783 cm^{-1}. MS (EI direct) m/z: M^+ 376. Anal. Calcd for $C_{19}H_{15}N_2O_3F_3 \cdot 0.1H_2O$: C, 60.35; H, 4.05; N, 7.41. Found: C, 60.31; H, 4.24; N, 7.34.

2.1.3. Synthesis of {2-[(4-cyclopropylpyridin-2-yl)carbonyl]-5-(trifluoromethyl)-1H-indol-3-yl}acetic acid **2**

*2.1.3.1. 4-(3-Chloropropyl)pyridine (**11**).* To a stirred solution of 4-pyridinepropanol **10** (Sigma–Aldrich, St. Louis, MO, USA, 13.72 g, 0.100 mol) in dry chloroform (Wako Pure Chemical Industries, Osaka, Japan, 50.0 mL) was added dropwise thionyl chloride (Wako Pure Chemical Industries, Osaka, Japan, 11.0 mL, 0.15 mol) at room temperature under N_2 over 40 min (corrosive gas evolution was observed). The resulting dark solution was stirred under reflux conditions under N_2 for 2 h, cooled to 0 °C, then basified by adding ice-cooled 50% aqueous KOH at 0 °C. The organic layer was separated, and the aqueous layer was extracted with chloroform (150 mL × 3) and CH_2Cl_2 (150 mL). The organic layers were combined, dried over anhydrous $MgSO_4$, filtered through a Celite pad, then concentrated *in vacuo* to afford the title product **11** as

15.55 g of a dark-brown oil as quantitative yield. ^{1}H NMR ($CDCl_3$, 270 MHz) δ 8.52 (2H, dd, J = 4.46 Hz, J = 1.65 Hz), 7.15–7.12 (2H, m), 3.53 (2H, t, J = 6.40 Hz), 2.79 (2H, t, J = 7.26 Hz), 2.15–2.05 (2H, m).

*2.1.3.2. 4-Cyclopropylpyridine (**12**).* To a solution of potassium *tert*-butoxide (Wako Pure Chemical Industries, Osaka, Japan, 11.67 g, 0.104 mol) in anhydrous THF (Dojindo Laboratories, Kumamoto, Japan, 200 mL) was added a solution of 4-(3-chloro)propylpyridine **11** (15.55 g, 0.100 mol) in anhydrous THF (100 mL) at room temperature under N_2 over 20 min. The reaction mixture was stirred at room temperature under N_2 for 29 h, then more potassium *tert*-butoxide (1.12 g, 10.0 mmol) was added to the mixture. The mixture was warmed up to 40 °C, stirred for 18 h, cooled to room temperature, then more potassium *tert*-butoxide (4.49 g, 40.0 mmol) was added. The mixture was warmed up to 40 °C, stirred for 18 h, and cooled to room temperature. The reaction mixture was poured into water (400 mL), extracted with a solution of chloroform (200 mL) and CH_2Cl_2 (800 mL). The organic layer was separated, dried over anhydrous $MgSO_4$, filtered, and concentrated *in vacuo* to afford 11.75 g of the title product **12** as a brown oil in 99% yield. ^{1}H NMR ($CDCl_3$, 270 MHz) δ 8.42 (2H, dd, J = 4.62 Hz, J = 1.65 Hz), 6.94 (2H, dd, J = 4.46 Hz, J = 1.65 Hz), 1.90–1.80 (1H, m), 1.12–1.04 (2H, m), 0.82–0.76 (2H, m)

*2.1.3.3. 4-Cyclopropylpyridine 1-oxide (**13**).* To a stirred solution of 4-cyclopropylpyridine **12** (11.75 g, 98.61 mmol) in glacial AcOH (84.5 mL) was added aqueous 30% H_2O_2 (Wako Pure Chemical Industries, Osaka, Japan, 14.1 mL, 124 mmol) at room temperature under N_2. The reaction mixture was warmed to 100 °C using an oil bath, stirred under N_2 for 12 h, removed from the oil bath, cooled to room temperature, then aqueous 30% H_2O_2 (8.0 mL) was added. Similarly, the mixture was stirred at 100 °C for 3 h, cooled to room temperature, then aqueous 30% H_2O_2 (8.0 mL) was added. Again, the mixture was stirred at 100 °C for 4 h, then aqueous 30% H_2O_2 (14.0 mL) was added at room temperature. The mixture was further stirred at 100 °C for 4 h, aqueous 30% H_2O_2 (14.0 mL) was added at room temperature, and then the mixture was stirred at 100 °C for 4 h. The resulting mixture was cooled to 0 °C, then saturated aqueous Na_2SO_3 was added at 0 °C to quench excess H_2O_2 until KI paper checking did not indicate the color change into brown or blue. The mixture was concentrated on a rotary evaporator followed by azeotropic evaporation with toluene. The residual solid was diluted with dry CH_2Cl_2 then added anhydrous K_2CO_3 (69.1 g, 500 mmol). The mixture was stirred for 3 h, allowed to stand overnight, then K_2CO_3 was filtered off. The filtrate was concentrated *in vacuo* to afford 10.85 g (purity 92%) of the title product **13** in net 75% yield, with small amount of compound **12** based on ^{1}H NMR analysis. ^{1}H NMR ($CDCl_3$, 270 MHz) δ 8.11–8.06 (2H, m), 6.97–6.92 (2H, m), 1.93–1.82 (1H, m), 1.17–1.10 (2H, m), 0.79–0.73 (2H, m).

*2.1.3.4. 4-Cyclopropylpyridine-2-carbonitrile (**14**).* To a stirred solution of 4-cyclopropylpyridine 1-oxide **13** (10.85 g, 73.22 mmol) in dry CH_2Cl_2 (150 mL) was added TMSCN (Tokyo Chemical Industry, Tokyo, Japan, 10.35 g, 104.3 mmol) and *N,N*-dimethylcarbamoyl chloride (Tokyo Chemical Industry, Tokyo, Japan, 8.90 mL, 96.3 mmol) at 0 °C under N_2. The reaction mixture was allowed to room temperature, stirred under N_2 for 27 h, then the resulting solution was cooled to 0 °C. A solution of anhydrous K_2CO_3 (40 g) in water (150 mL) was added to the above stirred solution at 0 °C. Then the organic layer was separated and the aqueous layer was extracted with CH_2Cl_2 (50 mL × 2). The organic layers were combined, washed with aqueous K_2CO_3, dried over anhydrous $MgSO_4$, filtered, and concentrated *in vacuo* to afford 18.57 g of the title product **14** as a brown oil (crude). ^{1}H NMR ($CDCl_3$, 270 MHz) δ 8.51 (1H, d, J = 5.29 Hz), 7.35 (1H, m), 7.16 (1H, dd, J = 5.27 Hz, J = 1.81 Hz), 1.98–1.88 (1H, m), 1.25–1.17 (2H, m), 0.89–0.83 (2H, m).

*2.1.3.5. 1-(4-Cyclopropylpyridin-2-yl)ethanone (**15**).* To a solution of 2-nitrile-4-cyclopropylpyridine **14** (18.57 g, crude) in dry benzene (Wako Pure Chemical Industries, Osaka, Japan, 130 mL)–anhydrous Et_2O (Wako Pure Chemical Industries, Osaka, Japan, 100 mL) was added dropwise 2 M solution of MeMgI/Et_2O (Tokyo Chemical Industry, Tokyo, Japan, 65.0 mL, 130 mmol) at 0 °C under N_2 over 1 h. The reaction mixture was warmed to room temperature, stirred under N_2 for 1 h, then cooled to 0 °C. Aqueous NH_4Cl (140 mL) was added dropwise to the mixture at 0 °C, warmed to room temperature, then stirred for 1 h. The aqueous layer was removed, and the organic layer was washed with water (140 mL), dried over anhydrous $MgSO_4$, filtered, and concentrated *in vacuo*. The residue was purified by flash column chromatography (silica gel, hexane/AcOEt = 3:1) to afford 6.367 g of the title product **15** a slight yellow oil in 54% yield (two steps). ^{1}H NMR ($CDCl_3$, 270 MHz) δ 8.49 (1H, d, J = 5.10 Hz), 7.69 (1H, d, J = 1.65 Hz), 7.15 (1H, dd, J = 5.10 Hz, J = 1.97 Hz), 2.71 (3H, s), 1.98–1.89 (1H, m), 1.17–1.10 (2H, m), 0.89–0.82 (2H, m).

*2.1.3.6. 2-Bromo-1-(4-cyclopropylpyridin-2-yl)ethanone (**16**). Typical procedure.* To a solution of 2-acetyl-4-cyclopropylpyridine **15** (1.290 g, 8.00 mmol) in 25% HBr/AcOH (15.0 mL) was added dropwise bromine (453 μL, 8.84 mmol) in glacial AcOH (2.0 mL) at 0 °C under N_2 over 20 min. The reaction solution was warmed to room temperature, then stirred under N_2 for 3 h. After some volume of the mixture was reduced *in vacuo*, the residue was cooled to 0 °C, basified by adding saturated aqueous $NaHCO_3$ at 0 °C. The mixture was extracted with Et_2O, and the ethereal layer was dried over anhydrous $MgSO_4$, filtered, then concentrated *in vacuo* to afford 1.896 g of the title product **16** as a brown oil in 99% yield. ^{1}H NMR ($CDCl_3$, 270 MHz) δ 8.48 (1H, d, J = 5.10 Hz), 7.73 (1H, d, J = 1.32 Hz), 7.19 (1H, dd, J = 5.10 Hz, J = 1.81 Hz), 4.84 (2H, s), 2.00–1.89 (1H, m), 1.20–1.10 (2H, m), 0.90–0.84 (2H, m).

*2.1.3.7. Methyl {2-[(4-cyclopropylpyridin-2-yl)carbonyl]-5-(trifluoromethyl)-1H-indol-3-yl}acetate (**17**).* A mixture of (2*E*)-3-{2-[(phenylsulfonyl)amino]-5-(trifluoromethyl)phenyl}acrylate **6** (2.146 g, 5.58 mmol), 2-bromo-1-(4-cyclopropylpyridin-2-yl)ethanone **16** (4.384 g, 18.3 mmol), and anhydrous K_2CO_3 (8.845 g, 64.0 mmol) in dry acetone (80.0 mL) was stirred at room temperature under N_2 for 24 h, then DBU (4.87 g, 32.0 mol) was added. The reaction mixture was stirred at room temperature under N_2 for 18 h then concentrated *in vacuo*. The residue was partitioned between AcOEt (100 mL) and H_2O (100 mL). The organic layer was separated and the aqueous layer was extracted with AcOEt (100 mL × 2). The organic layers were combined, dried over anhydrous $MgSO_4$, filtered, then concentrated *in vacuo*. The residue was purified by flash column chromatography (silica gel, hexane/AcOEt = 3:1) to afford 578.1 mg of the title product **17** in 26% yield as a yellow solid. ^{1}H NMR ($CDCl_3$, 270 MHz) δ 12.74 (1H, br s), 8.57 (1H, d, J = 5.10 Hz), 7.99–7.96 (2H, m), 7.58–7.56 (2H, m), 7.24 (1H, dd, J = 5.27 Hz, J = 1.97 Hz), 4.33 (2H, s), 3.75 (3H, s), 2.03–1.93 (1H, m), 1.23–1.16 (2H, m), 0.95–0.89 (2H, m).

*2.1.3.8. {2-[(4-Cyclopropylpyridin-2-yl)carbonyl]-5-(trifluoromethyl)-1H-indol-3-yl}acetic acid (**2**).* A mixture of methyl [2-(4-cyclopropylbenzoyl)-5-(trifluoromethyl)-1*H*-indol-3-yl]acetate **17** (578.1 mg, 1.437 mmol) and 2 N NaOH (3.0 mL, 6.0 mmol) in MeOH (Wako Pure Chemical Industries, Osaka, Japan, 30 mL)–THF (Wako Pure Chemical Industries, Osaka, Japan, 30 mL) was stirred under reflux conditions under N_2, stirred for 5 h, cooled to room temperature, then 2 N HCl (3.0 mL) was added. The mixture was

concentrated *in vacuo*, and the residue was dissolved in anhydrous THF (Dojindo Laboratories, Kumamoto, Japan), dried over anhydrous $MgSO_4$, filtered, then concentrated *in vacuo*. The residue was recrystallized from AcOEt–hexane to afford 518.2 g of the title product **2** in 93% yield as a yellow solid. Mp: 212.7 °C. ^{1}H NMR (DMSO-d_6, 270 MHz) δ 12.50 (1H, br s), 12.20 (1H, br s), 8.63 (1H, d, J = 5.10 Hz), 8.22 (1H, s), 7.85–7.79 (2H, m), 7.58 (1H, d, J = 9.07 Hz), 7.43 (1H, dd, J = 5.10 Hz, J = 1.81 Hz), 4.14 (2H, s), 2.17–2.07 (1H, m), 1.18–1.11 (2H, m), 0.94–0.88 (2H, m). IR (KBr): 3238, 1717, 1651, 1597, 1541, 1420, 1335, 1279, 1215, 1186, 1165, 1101, 1049, 1028, 907, 889, 818 cm^{-1}. MS (EI direct) m/z: M$^+$ 388. Anal. Calcd for $C_{20}H_{15}N_2O_3F_3$: C, 61.70; H, 4.26; N, 6.95. Found: C, 61.86; H, 3.89; N, 7.21.

2.1.4. Synthesis of {6-chloro-2-[(4-cyclopropylpyridin-2-yl)carbonyl]-1H-indol-3-yl}acetic acid 3

2.1.4.1. Methyl 3-{4-chloro-2-[(phenylsulfonyl)amino]phenyl}acrylate (19). To a stirred solution of methyl 3-(2-amino-4-chlorophenyl)acrylate **18** (synthesized at Pfizer Global Research & Development, Aichi, Japan, according to the reported procedure [57], 37.5 g, 0.177 mmol) and dry pyridine (42.9 mL, 0.530 mmol) in dry CH_2Cl_2 (500 mL) was added dropwise benzenesulfonyl chloride (Tokyo Chemical Industry, Tokyo, Japan, 24.9 mL, 0.195 mmol) under N_2 at room temperature. The reaction mixture was stirred at room temperature under N_2 for 14 h, then MeOH was added, stirred for 30 min, and then concentrated *in vacuo*. The residue was dissolved in CH_2Cl_2 (500 mL), washed with 2 N HCl (300 mL × 2) and brine, dried over anhydrous $MgSO_4$, filtered, and concentrated *in vacuo*. The resulting solid was diluted with AcOEt (800 mL), and then filtered. The filtrate was concentrated *in vacuo*. The resulting solid was recrystallized from dry EtOH (300 mL) to afford 49.2 g of the title product **19** in 79% yield as a slight brown crystalline. ^{1}H NMR (270 MHz, $CDCl_3$) δ 7.75–7.72 (2H, m), 7.58–7.36 (6H, m), 7.20 (1H, dd, J = 8.56 Hz, J = 2.13 Hz), 7.14 (1H, br s), 6.15 (1H, d, J = 15.8 Hz), 3.78 (3H, s).

2.1.4.2. Methyl {6-chloro-2-[(4-cyclopropylpyridin-2-yl)carbonyl]-1H-indol-3-yl}acetate (20). A mixture of methyl 3-{4-chloro-2-[(phenylsulfonyl)amino]phenyl}acrylate **19** (2.287 g, 6.50 mmol), 2-bromo-1-(4-cyclopropylpyridin-2-yl)ethanone **16** (1.896 g, 7.90 mmol), and anhydrous K_2CO_3 (6.29 g, 45.5 mmol) in dry acetone (60.0 mL) was stirred at room temperature under N_2 for 15 h, then DBU (3.96 g, 26.0 mmol) was added. The reaction mixture was stirred at room temperature under N_2 for 7 h then concentrated *in vacuo*. The residue was partitioned between AcOEt (50 mL) and H_2O (50 mL). The organic layer was separated and the aqueous layer was extracted with AcOEt (50 mL × 3). The organic layers were combined, dried over anhydrous $MgSO_4$, filtered, and concentrated *in vacuo*. The residue was purified by flash column chromatography (silica gel, hexane/AcOEt/CH_2Cl_2 = 18:3:2) to afford 686.0 mg of the title product **20** in 29% yield as a yellow solid. ^{1}H NMR ($CDCl_3$, 270 MHz) δ 12.54 (1H, br s), 8.56 (1H, d, J = 5.10 Hz), 7.97 (1H, d, J = 1.81 Hz), 7.62 (1H, d, J = 8.72 Hz), 7.52–7.51 (1H, m), 7.23 (1H, dd, J = 5.10 Hz, J = 1.81 Hz), 7.12 (1H, dd, J = 8.56 Hz, J = 1.81 Hz), 4.30 (2H, s), 3.73 (3H, s), 2.03–1.93 (1H, m), 1.22–1.15 (2H, m), 0.95–0.89 (2H, m).

2.1.4.3. {6-Chloro-2-[(4-cyclopropylpyridin-2-yl)carbonyl]-1H-indol-3-yl}acetic acid (3). A solution of methyl {6-chloro-2-[(4-cyclopropylpyridin-2-yl)carbonyl]-1*H*-indol-3-yl}acetate **20** (664.5 mg, 1.80 mmol) in MeOH (40 mL)–THF (35 mL) was added 2 N NaOH (4.5 mL, 9.0 mmol) at room temperature under N_2. The reaction mixture was warmed up to reflux conditions using an oil bath (~110 °C), stirred under N_2 for 3 h then cooled to room temperature. 2 N HCl (4.5 mL) was added to the reaction solution, then the mixture was concentrated *in vacuo*. The residue was dissolved in anhydrous THF (Dojindo Laboratories, Kumamoto, Japan), dried over anhydrous $MgSO_4$, filtered, and concentrated *in vacuo*. The resulting solid was washed with AcOEt to afford 570.0 mg of the title product **3** in 89% yield as yellow solid. Mp: 214 °C. ^{1}H NMR (DMSO-d_6, 270 MHz) δ 12.28 (1H, br s), 12.26 (1H, br s), 8.64 (1H, d, J = 5.10 Hz), 7.80–7.73 (3H, m), 7.44 (1H, dd, J = 5.10 Hz, J = 1.81 Hz), 7.11 (1H, dd, J = 8.72 Hz, J = 1.84 Hz), 4.08 (2H, s), 2.18–2.08 (1H, m), 1.20–1.13 (2H, m), 0.95–0.89 (2H, m). IR (KBr): 3250, 1711, 1641, 1595, 1533, 1281, 1250, 1209, 1184, 1144, 1059, 1003, 891 cm^{-1}. MS (EI direct) m/z: M$^+$ 354. Anal. Calcd for $C_{19}H_{15}N_2O_3Cl{\cdot}0.1H_2O$: C, 64.00; H, 4.54; N, 7.56. Found: C, 64.00; H, 4.30; N, 7.86.

2.2. Biology

2.2.1. Materials

Human umbilical vein endothelial cells (HUVECs) were purchased from Morinaga Institute (Yokohama, Japan). Recombinant human IL-1β was purchased from R&D Systems (Minneapolis, MN, USA). A23187 (calcium ionophore), LPS (from *Escherichia coli* 0111:B4), and indomethacin were purchased from Sigma–Aldrich (St. Louis, MO, USA). PGE_2 and TXB_2 were purchased from Cayman Chemical (Ann Arbor, MI, USA). Sodium heparin (Novo-Heparin) was purchased from Novo Nordisk A/S (Bagsværd, Denmark). λ-Carrageenan (Picnin-A) was purchased from Zushikagaku (Zushi, Kanagawa, Japan). Radioimmunoassay (RIA) kit was purchased from Amersham (Buckinghamshire, United Kingdom). Test compounds **1**–**3** were prepared by us at Pfizer Global Research & Development, Nagoya Laboratories (Aichi, Japan), and the purities of them were confirmed by elementary analysis to be within ±0.4% of calculated values, respectively (see Section 2.1). The compounds **1**–**3** were used for pharmacological evaluations as free acids, respectively. All other chemicals were obtained from Wako Pure Chemical Industries (Osaka, Japan) unless stated otherwise. All common chemicals were analytical or the highest available grade.

2.2.2. In vitro characterization of COX-2 inhibitors

2.2.2.1. Human cell-based COX-1 assay. Platelets were prepared from human peripheral blood obtained from healthy adult volunteers under informed consent. Fresh blood was collected into vacutainers (Becton Dickinson, Franklin Lakes, NJ, USA) containing 1/10 volume of anticoagulant solution (3.8% sodium citrate), and centrifuged at 200 × g for 10 min. The supernatant (platelet-rich plasma) was mixed with 50% volume of 0.14 M NaCl containing 12 mM Tris–HCl, 1.2 mM EDTA, pH 7.4. This mixture was centrifuged at 750 × g for 10 min, and the pellet was suspended in platelet buffer (Ca^{2+}-free Hanks buffer containing 20 mM HEPES, pH 7.4 and 0.2% BSA). After centrifugal washing with the platelet buffer, the resulting pellet, referred to as human washed platelets (HWPs), was resuspended in the platelet buffer at a cell concentration of 2.85 × 10^8 cells/mL, then stored at room temperature until use. Immediately prior to assay, 10 μL of 12.6 mM $CaCl_2$ was added to 70 μL HWPs suspension (2.0 × 10^7 cells/mL in a 96-well U bottom plate). Platelets were preincubated in the absence or presence of 10 μL of test compound dissolved in DMSO at final concentrations varying 0.01–10 μM (final concentration, less than 0.1%) for 20 min before stimulation with 10 μL of calcium ionophore A23187 (final concentration, 10 μM). After further 15 min incubation at 37 °C with A23187, the reaction was stopped by the addition of EDTA (final concentration, 7.7 mM), and the reaction medium was quantitated for TXB_2 by a radioimmunoassay (RIA) kit (Amersham, Buckinghamshire, United Kingdom) according to the manufacturer's procedure [58].

2.2.2.2. Human cell-based COX-2 assay. The human cell based COX-2 assay was carried out as previously described [59]. Confluent human umbilical vein endothelial cells (HUVECs) (2×10^4 cells/well) in a 96-well plate were washed with 100 μL of RPMI-1640 containing 2% fetal calf serum (FCS), and incubated with 300 U/mL of recombinant human IL-1β for 24 h at 37 °C for induction of COX-2. After washing with Hanks buffer containing 20 mM HEPES, pH 7.4 and 0.2% BSA, HUVECs were preincubated in Hanks buffer containing 20 mM HEPES, pH 7.4 and 0.2% BSA, with or without 10 μL of test compound dissolved in DMSO at final concentrations varying 1 nM to 1 μM (final concentration, less than 0.1%) for 20 min before stimulation with 30 μM of A23187. After further 15 min incubation at 37 °C with A23187, the reaction medium was quantitated for 6-keto-prostaglandin $F_{1\alpha}$ (6-keto-$PGF_{1\alpha}$), that is, spontaneously degraded stable form of PGI_2, by a RIA kit (Amersham, Buckinghamshire, United Kingdom).

2.2.2.3. Human whole blood COX-1 assay. Human peripheral blood obtained from healthy adult volunteers under informed consent was collected into vacutainers containing 143 USP units of sodium heparin. Aliquots of 80 μL of the heparinized blood was dispensed in a 96-well U-bottom plate containing 10 μL of test compound dissolved in DMSO at final concentrations varying 0.1–100 μM (final concentration, less than 0.1%), and incubated with 10 μL of A23187 (final concentration, 30 μM) for 30 min at 37 °C. The reaction was stopped by centrifugation at 400 × *g* for 5 min at 4 °C, and the supernatant was quantitated for TXB_2 by a RIA kit (Amersham, Buckinghamshire, United Kingdom) [60,61].

2.2.2.4. Human whole blood COX-2 assay. Human peripheral blood obtained from healthy adult volunteers under informed consent was collected into vacutainers (Falcon®; Becton Dickinson, Franklin Lakes, NJ, USA) containing 143 USP units of sodium heparin (Novo-Heparin). Aliquots of 80 μL of the heparinized blood was dispensed in a 96-well U-bottom plate containing 10 μL of test compound dissolved in DMSO at final concentrations varying 0.1–100 μM (final concentration, less than 0.1%), and incubated with 10 μL of lipopolysaccharide (LPS, from *E. coli* 0111:B4, final concentration, 30 μg/mL) for 24 h at 37 °C for induction of COX-2. The reaction was stopped by centrifugation at 400 × *g* for 5 min at 4 °C, and the supernatant was quantitated for PGE_2 by RIA kit (Amersham, Buckinghamshire, United Kingdom) [60–62].

2.2.3. In vivo studies

2.2.3.1. General. All animal experiments were conducted according to the guideline of animal care and use, and all procedures were approved by the Animal Ethics Committee in Pfizer Global Research & Development, Nagoya Laboratories. The animal work was also approved by the Pfizer Institutional Animal Care and Use Committee (IACUC).

2.2.3.2. LPS-induced pyresis in SPF/VAF male F344 rats. Specific pathogen free and virus antibody free (SPF/VAF) male Fischer 344 (F344) rats (F344/DuCrj, 5 weeks old, 75–95 g, Charles River Laboratories, Japan Inc., Atsugi, Japan) were fasted for 20 h before use. At approximately 9:00 A.M., the basal rectal temperature was recorded using a digital thermometer (DT-300; Inter Medical Co. Ltd., Nagoya, Japan). Immediately (at time zero), the rats were injected intraperitoneally with either LPS (from *E. coli* 0111:B4, 0.25 mg/kg) or saline. Then the rectal temperature was measured again at 5 and 7 h after the LPS injection. After the measurement at 5 h when the increase in rectal temperature had reached a plateau, the LPS-injected rats were given orally either the vehicle (0.1% (v/v) methylcellulose in distilled water) or a test compound at given dose in a volume of 1 mL/100 g body weight.

The changes in the body temperature from 0 h (predose) to 7 h (postdose) for vehicle-treated control group and basal group were calculated, respectively, and the mean values of compound-treated group were compared to that of the vehicle-treated group to determine the percent inhibition of fever as the following equation:

$$\%\text{Inhibition} = \frac{\Delta\text{Temp}_{\text{vehicle control}} - \Delta\text{Temp}_{\text{drug treatement}}}{\Delta\text{Temp}_{\text{vehicle control}} - \Delta\text{Temp}_{\text{basal}}} \times 100,$$

ΔTemp is change in body temperature from 0 to 7 h.

A dose that gave half-maximal effect (ED_{50}) was calculated over a dose range of 0.3, 1.0, 3.0, and 10 mg/kg for oral administration of the test compound with linear-regression analysis plotted on a semilog scale.

2.2.3.3. Carrageenan-induced foot-edema formation in SPF/VAF male SD rats. SPF/VAF male Sprague–Dawley (SD) rats (Crj:CD(SD), 5 weeks old, 110–130 g, Charles River Laboratories, Japan Inc., Hino, Japan) that were fasted overnight were injected intraplantarly with 0.1 mL of a 1% (w/v) λ-carrageenan (Picnin-A) suspension in saline into the right hind paw as previously reported [63–65]. Either the vehicle (5% (v/v) Tween 80 in distilled water) or a test compound was dosed orally in a volume of 1 mL/100 g body weight at 1 h before carrageenan injection. Foot volume was measured by a water displacement plethysmometer (Unicom Co., Yachiyo, Japan) before and 3 h after carrageenan injection. The increases in foot volume for 3 h were calculated. Foot edema was compared with vehicle-control group, and the percent inhibition was calculated taking the values in the control group as 0%. A dose that gave 40% effect (ED_{40}) was calculated over a dose range of 0.3, 1.0, and 3.0 mg/kg for oral administration of the test compound with linear-regression analysis plotted on a semilog scale.

2.2.3.4. PGE_2 production in carrageenan-induced edema site of SPF/VAF male SD rats. Determination of PGE_2 synthesized in the inflammatory site was carried out essentially according to a previously described method [66]. Foot edema in SPF/VAF male SD rats (Crj:CD(SD), 5 weeks old, 110–130 g) was induced by intraplantar injection of a 1% (w/v) λ-carrageenan suspension. The measurement of inhibitory activity against carrageenan-induced foot edema for the test compound, that was administrated orally at 1 h before carrageenan injection, was performed at 3 h after carrageenan injection (see Section 2.2.3.3). And then immediately, the animals were euthanized and sacrificed by cervical dislocation. The foot was amputated, frozen in liquid nitrogen, and stored at–80 °C until analysis. The frozen foot was crushed, mixed with 7 mL of ethanol containing 10 μg/mL of indomethacin to inhibit PGE_2 production during further handling, pulverized in a Waring blender, and clarified by centrifugation at 2000 × *g* for 10 min at 4 °C. PGE_2 was extracted by a Sep-Pak C18 cartridge (Waters Corporation, Milford, MA, USA), and dried in vacuum. Samples were diluted to a final volume of 0.5 mL with assay buffer (50 mM Tris/HCl, pH 7.4 containing 0.9% NaCl, 0.01% Triton X-100 and 0.1% (w/v) bactogelatin) and the levels of PGE_2 were determined by RIA according to the manufacture's direction (RIA kit, Amersham, Buckinghamshire, United Kingdom). Either the vehicle (5% (v/v) Tween 80 in distilled water) or the test compound was dosed orally in a volume of 1 mL/100 g body weight 1 h before carrageenan injection as already described in Section 2.2.3.3. The mean values of compound-treated group were compared to that of vehicle-treated control group to determine the percent inhibition of PGE_2 production as the following equation:

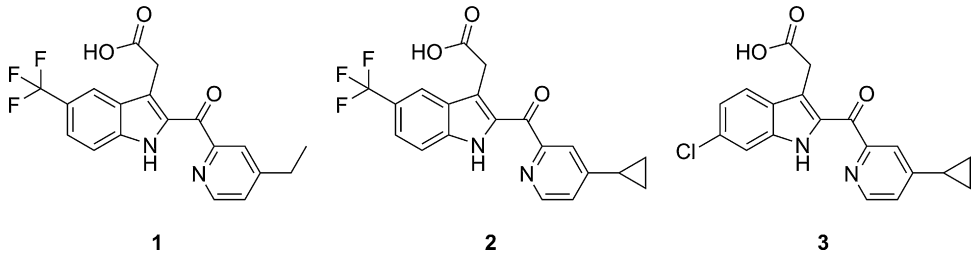

Fig. 1. Structures of novel orally potent acid-type COX-2 inhibitors: compound **1**: {2-[(4-ethylpyridin-2-yl)carbonyl]-5-(trifluoromethyl)-1*H*-indol-3-yl}acetic acid; compound **2**: {2-[(4-cyclopropylpyridin-2-yl)carbonyl]-5-(trifluoromethyl)-1*H*-indol-3-yl}acetic acid; compound **3**: {6-chloro-2-[(4-cyclopropylpyridin-2-yl)carbonyl]-1*H*-indol-3-yl}acetic acid.

$$\%\,\text{Inhibition} = \frac{\text{PGE}_2\ \text{content}_{\text{vehicle control}} - \text{PGE}_2\ \text{content}_{\text{drug treatement}}}{\text{PGE}_2\ \text{content}_{\text{vehicle control}} - \text{PGE}_2\ \text{content}_{\text{basal}}} \times 100.$$

2.2.4. Statistical analysis

Values are presented as mean ± standard error of the mean (S.E.M.). For *in vitro* assays, inhibitory concentration at 50% inhibition (IC_{50}) was determined from a dose curve run in duplicate unless otherwise stated. For *in vivo* assays, statistical comparisons of experimental data were performed by one-way ANOVA followed by Dunnett's multiple comparison tests or two-tailed unpaired *t*-test when appropriate. For all statistical tests, differences were regarded statistically significant when the *P*-value was less than 0.05. Numerical data were analyzed using GraphPad Prism 4.0 software (GraphPad Software, Inc., San Diego, CA, USA).

2.3. Physicochemistry

The lipophilicity values of COX-2 inhibitors were estimated as values of ACD log $D_{7.4}$, the octanol–water distribution coefficient for ionizable compounds at pH 7.4, calculated by ACD software, ACD/Laboratories 9.0 (Advanced Chemistry Development, Inc., Ontario, Canada).

3. Results

3.1. Chemistry

Novel COX-2 inhibitor [2-{[(4-substituted)-pyridin-2-yl]carbonyl}-(6- or 5-substituted)-1*H*-indol-3-yl]acetic acid derivatives **1**–**3** (Fig. 1) were prepared as shown in Figs. 2–4.

Thus, compound **1** was prepared as follows (Fig. 2). First, Heck–Mizoroki reaction for 2-bromo-4-(trifluoromethyl)aniline **4** and methyl acrylate was performed with catalytic amount of $Pd(OAc)_2$ and tri(*o*-tolyl)phosphine to prepare methyl (2*E*)-3-[2-amino-5-(trifluoromethyl)phenyl]acrylate **5** [67,68]. Then the acrylate derivative **5** with benzenesulfonyl chloride was led to phenyl aminosulfonate **6**. Second, 1-(4-ethylpyridin-2-yl)ethanone **7** [55,56] was brominated with bromine in HBr/AcOH condition to form 2-bromo-1-(4-ethylpyridin-2-yl)ethanone **8** [69]. Third, Michael addition reaction for the methyl acrylate derivative **6** and the 2-bromo-1-ethanone derivative **8** was

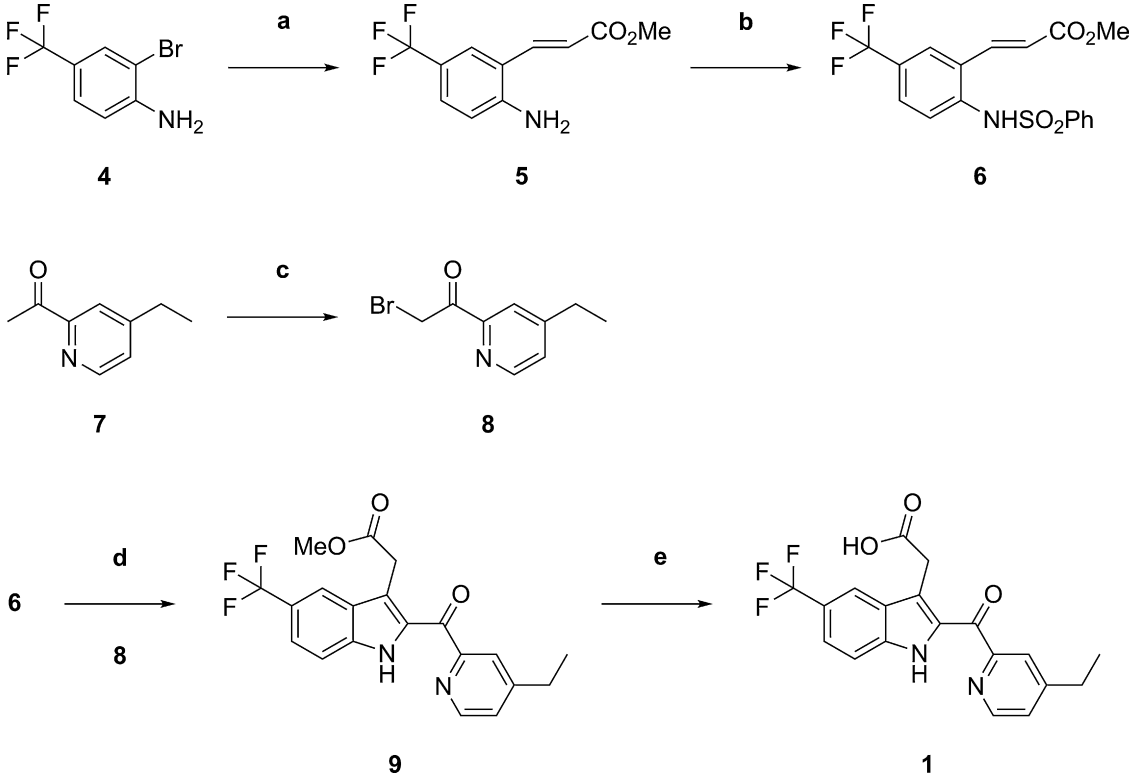

Fig. 2. Synthesis of compound **1**. *Reagents and conditions*: (a) methyl acrylate, $Pd(OAc)_2$, $P(o\text{-Tol})_3$, Et_3N, CH_3CN, reflux; (b) $PhSO_2Cl$, pyridine, CH_2Cl_2; (c) Br_2/AcOH, 25% HBr/AcOH, 0 °C to room temperature; (d) K_2CO_3, acetone; then DBU; (e) 2 N NaOH, EtOH, reflux; then 2 N HCl, room temperature.

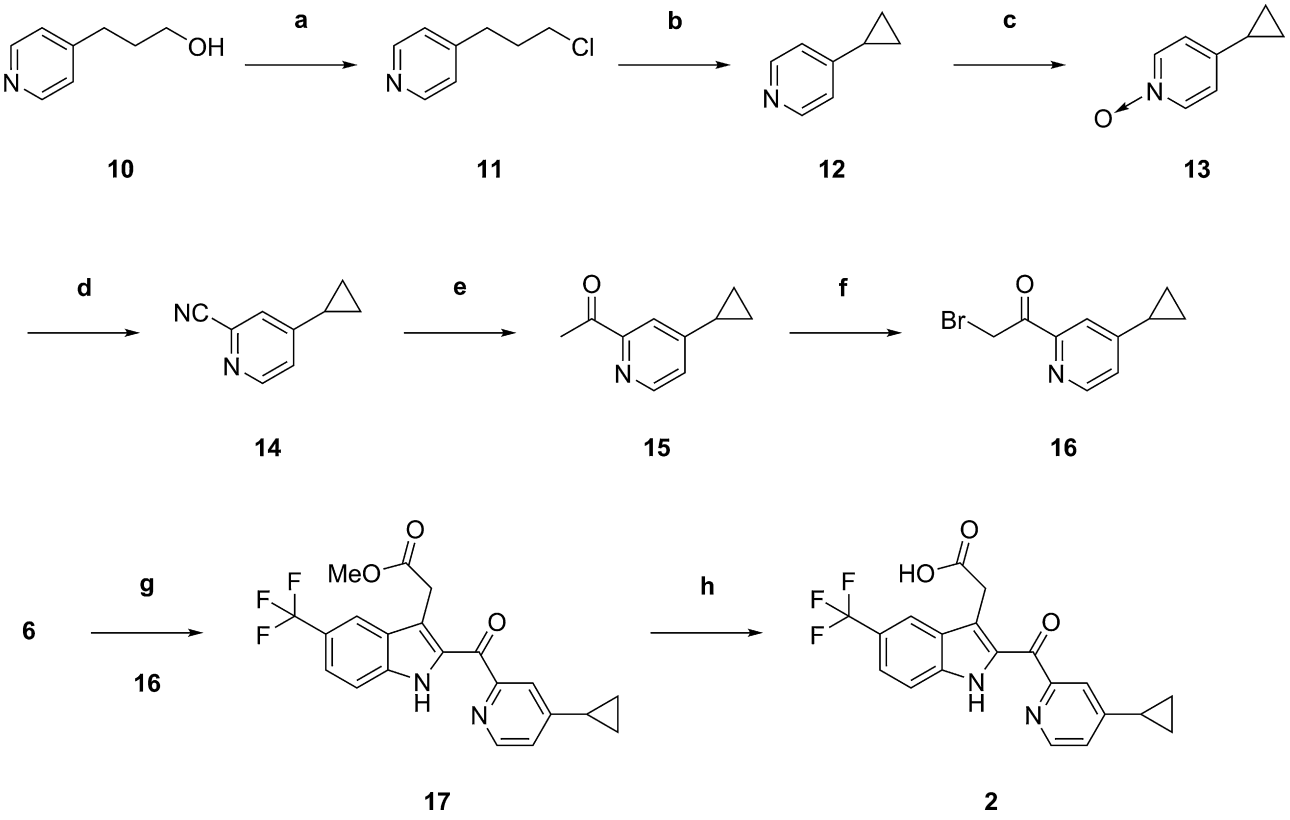

Fig. 3. Synthesis of compound **2**. *Reagents and conditions*: (a) $SOCl_2$, $CHCl_3$, room temperature to reflux; (b) *t*-BuOK, THF, room temperature to 40 °C; (c) aqueous 30% H_2O_2, AcOH, room temperature to 100 °C; (d) TMSCN, *N*,*N*-dimethylcarbamoyl chloride, CH_2Cl_2, 0 °C to room temperature; (e) 2 M MeMgI/Et_2O, PhH–Et_2O, 0 °C to room temperature; (f) Br_2/AcOH, 25% HBr/AcOH, 0 °C to room temperature; (g) K_2CO_3, acetone; then DBU; (h) 2 N NaOH, MeOH–THF, reflux; then 2 N HCl, room temperature.

performed with K_2CO_3 to form indoline skeleton, followed by dephenylsulfonation-assisted one-pot aromatization of the indoline by 1,8-diazabicyclo[5.4.0]undec-7-ene (DBU) to afford indole form, methyl {2-[(4-ethylpyridin-2-yl)carbonyl]-5-(trifluoromethyl)-1*H*-indol-3-yl}acetate **9**. Finally, the methyl ester portion was hydrolyzed to afford requisite {2-[(4-ethylpyridin-2-yl)carbonyl]-5-(trifluoromethyl)-1*H*-indol-3-yl}acetic acid **1** as a sole product.

Next, compound **2** was prepared as follows (Fig. 3). 4-Chloropropylpyridine **11**, prepared from 4-hydroxypropylpyridine **10** by chlorination, was treated with potassium *tert*-butoxide to afford 4-cyclopropylpyridine **12** by intra-nucleophilic cyclopropanation reaction [70]. Treatment of compound **12** with H_2O_2 gave N-oxidized product **13**, followed by 2-selective nitrilation by modified Reissert–Henze reaction to afford 4-cyclopropylpyridine-2-carbonitrile **14** [71]. The 2-nitrile moiety was converted into 2-acetyl group by treatment with MeMgI [55] to give 2-acetyl-4-cycloproylpyridine **15**, which was brominated to afford 2-bromo-1-(4-cyclopropylpyridin-2-yl)ethanone **16**. Subsequently, indole skeleton was constructed from compounds **6** and **16** to form

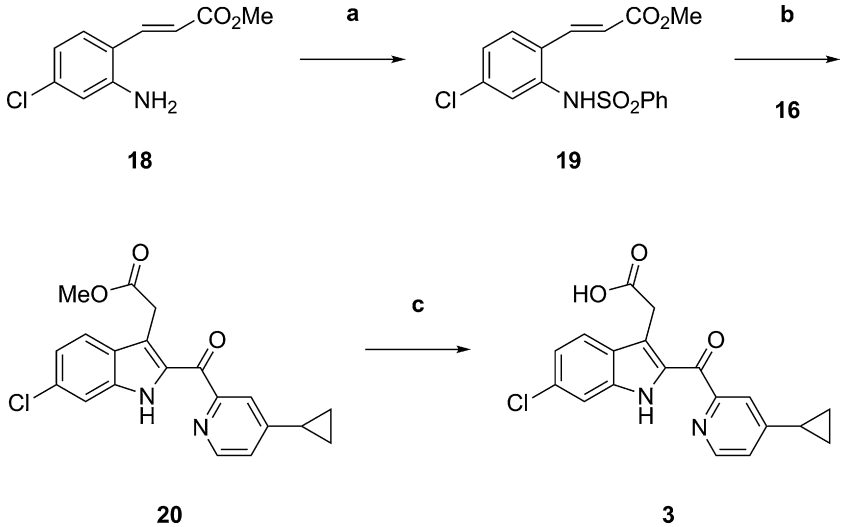

Fig. 4. Synthesis of compound **3**. *Reagents and conditions*: (a) $PhSO_2Cl$, pyridine, CH_2Cl_2; (b) K_2CO_3, acetone; then DBU; (c) 2 N NaOH, MeOH–THF, room temperature to reflux; then 2 N HCl, room temperature.

Table 2
In vitro inhibitory effects of compounds 1–3 against COX-2/COX-1 activities.[a]

Compounds	Human cell assay		HWB assay	
	COX-2[b]	COX-1[c]	COX-2[d]	COX-1[e]
	6-keto-$PGF_{1\alpha}$ (HUVECs), IC_{50} (μM)	TXB_2 (HWPs), IC_{50} (μM)	PGE_2 IC_{50} (μM)	TXB_2, IC_{50} (μM)
1	0.00229 ± 0.00026[f]	3.618 ± 0.715[g]	0.331 ± 0.094[g]	42.00 ± 16.60[g]
2	0.0522 ± 0.0286[g]	7.890[h]	0.635 ± 0.535[g]	>100[g]
3	0.0187 ± 0.0022[g]	5.766[h]	2.500 ± 1.100[g]	>100[g]

[a] Data are expressed as the mean ± S.E.M.
[b] IC_{50} values of compounds against COX-2 activity were determined as inhibitory activity against 6-keto-prostaglandin $F_{1\alpha}$ synthesis in human umbilical vein endothelial cells (HUVECs) that were expressing COX-2 by interleukin-1β (IL-1β)-stimulation.
[c] IC_{50} values of compounds against COX-1 activity were determined as inhibitory activity against thromboxane B_2 production in human washed platelets (HWPs).
[d] IC_{50} values of compounds against COX-2 activity were determined as inhibitory activity against prostaglandin E_2 synthesis in human whole blood (HWB) that was expressing COX-2 by lipopolysaccharide (LPS)-stimulation.
[e] IC_{50} values of compounds against COX-1 activity were determined as inhibitory activity against thromboxane B_2 production in HWB.
[f] $n = 9$, as number of independent experiments.
[g] $n = 2$, as number of independent experiments.
[h] $n = 1$, as number of independent experiments.

methyl [2-(4-cyclopropylbenzoyl)-5-(trifluoromethyl)-1*H*-indol-3-yl]acetate **17** in the same manner for compound **9**, which was hydrolyzed to form [2-(4-cyclopropylbenzoyl)-5-(trifluoromethyl)-1*H*-indol-3-yl]acetic acid **2** as a sole product.

Also, compound **3** was prepared as follows (Fig. 4). Methyl 3-(2-amino-4-chlorophenyl)acrylate **18** was prepared by Wittig reaction of 1-chloro-3-nitro-4-benzaldehyde and the reduction of the nitro group to convert into amino group [57]. Then the resulting methyl acrylate derivative **18** was led to corresponding phenyl aminosulfonate **19**. According to the above way to construct indole skeleton, compounds **19** and **16** were converted into methyl {6-chloro-2-[(4-cyclopropylpyridin-2-yl)carbonyl]-1*H*-indol-3-yl}acetate **20**, followed by hydrolysis to form {6-chloro-2-[(4-cyclopropylpyridin-2-yl)carbonyl]-1*H*-indol-3-yl}acetic acid **3** as a sole product.

The purities of the compounds **1**–**3** were confirmed by elementary analysis to be within ±0.4% of calculated values, respectively. All of these [2-{[(4-substituted)-pyridin-2-yl]carbonyl}-(6- or 5-substituted)-1*H*-indol-3-yl]acetic acids **1**–**3** were used for SAR study with pharmacological evaluations as free acids, respectively.

3.2. Structure–activity relationships of COX-2 inhibitors

3.2.1. In vitro activity and selectivity against COX isoforms

First, as structure–activity relationship (SAR) study of COX-2 inhibitor *in vitro*, various types of [2-{[(4-substituted)-pyridin-2-yl]carbonyl}-(6- or 5-substituted)-1*H*-indol-3-yl]acetic acid derivatives were designed, synthesized, and evaluated. The *in vitro* activity and selectivity as a COX-2 inhibitor for the respective compounds were evaluated by the measurements of inhibitory activities against actions of COX isozymes, that is, constitutional COX-1 and inducible COX-2, in human cells or in human whole blood (HWB). Hence, as human cellular assays, the inhibitory activities of the compounds were determined (i) on TXB_2 production in the human washed platelets (HWPs) to investigate COX-1 inhibition, and (ii) on 6-keto-prostaglandin $F_{1\alpha}$ (6-keto-$PGF_{1\alpha}$, spontaneously degraded stable form of PGI_2) production in the human umbilical vein endothelial cells (HUVECs), that were expressing COX-2 induced by IL-1β, to investigate COX-2 inhibition, respectively [58,59]. Also, as HWB assays, the inhibitory activities of the compounds were determined (i) on TXB_2 production in HWB to investigate COX-1 inhibition, and (ii) on PGE_2 production in HWB, that was expressing COX-2 induced by LPS, to investigate COX-2 inhibition, respectively [58,60–62].

It is reported that COX-1 exhibits a low level of expression in HUVECs as an exception of its ubiquitous localization in body, while COX-2 is absent or expressed low levels in HUVECs, human platelets, and human blood monocytes as other most tissues at normal stages [28]. The level of COX-2 induced by IL-1β- or LPS-stimulation in HUVECs or in human monocytes is very high, compared to a neglectable or low level of COX-1 that is not affected by IL-1β- or LPS-stimulation in the HUVECs [28,72] or by LPS-stimulation in the human monocytes [3]. In our study condition for the present HUVEC assays, almost no 6-keto-$PGF_{1\alpha}$ production was observed without IL-1β-stimulation (not shown). Therefore it was estimated that the increased 6-keto-$PGF_{1\alpha}$ production in HUVECs by IL-1β-stimulation was derived from induced-COX-2 and not derived from constitutive COX-1 in the present study. As well, the increased PGE_2-production in human monocytes by LPS-stimulation is explained as COX-2 induction-dependent response [73].

The results of the respective inhibitory activities for compounds **1**–**3** in the human cellular and HWB studies are shown in Table 2, and the dose-dependent inhibitory activities for the compounds in the HUVEC study are shown in Fig. 5. For selectivity indices of human COX-2 inhibitor in the present study *in vitro*, COX-2-inhibition selectivity was estimated as IC_{50} against COX-2 over IC_{50} against COX-1 in the human cellular studies and HWB studies, respectively.

Actually, in COX-2-induced HUVEC assays, compounds **1**–**3** displayed highly potent inhibition on 6-keto-$PGF_{1\alpha}$ production (IC_{50} = 0.00229–0.0522 μM); and in COX-2-induced HWB assays, compounds **1**–**3** showed highly potent inhibition on PGE_2 production (IC_{50} = 0.331–2.500 μM), respectively. By contrast, in HWP assays, compounds **1**–**3** showed less potent inhibition on TXB_2 production (IC_{50} = 3.618–7.890 μM); and in HWB assays, the

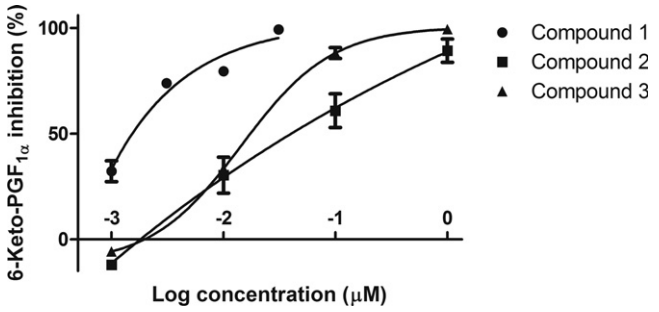

Fig. 5. *In vitro* inhibitory effects of compounds **1**–**3** against COX-2 activity in HUVECs. The inhibitory effects of compounds **1**–**3** against COX-2 activity were determined as inhibitory activity against 6-keto-prostaglandin $F_{1\alpha}$ synthesis in human umbilical vein endothelial cells (HUVECs) that were expressing COX-2 by IL-1β-stimulation. The results for compound **1** were mean for two independent experiments out of nine. The results for compounds **2** and **3** were mean for two independent experiments, respectively. Data are expressed as the mean ± S.E.M.

Table 3
In vivo oral anti-pyretic and anti-inflammatory effects of COX-2 inhibitors **1–3** in pyresis and edema models of rats.

Compounds[d]	Oral anti-pyretic effect[a] (Male F344 rats)		Oral anti-inflammatory effect[b] (Male SD rats)		Oral suppressive effect on PGE_2 production[c] (Male SD rats)
	%Inhibition		%Inhibition		%Inhibition
	At 10 mg/kg	ED_{50}[e]	At 3 mg/kg	ED_{40}[f]	At 3 mg/kg
Control	0.00 ± 5.60	–	0.00 ± 5.48	–	0.00 ± 15.98
1	78.17 ± 5.13***	1.68 mg/kg	45.68 ± 6.61**	2.07 mg/kg	88.16 ± 5.09**
2[g]	51.88 ± 3.32***	–	Not tested	–	Not tested
3[g]	70.73 ± 7.99***	–	Not tested	–	Not tested

***$p < 0.001$, **$p < 0.01$, significant difference from the control group analyzed by one-way ANOVA followed by Dunnett's multiple comparison tests for compound **1**, and analyzed by two-tailed unpaired *t*-tests for compounds **2** and **3**, respectively. The results of compound **1** were obtained from dose response experiments, and the results of compounds **2** and **3** were obtained from single dose experiments, respectively.

[a] Oral inhibitory effect of COX-2 inhibitors **1–3** against fever by LPS in SPF/VAF male F344 rats. LPS was intraperitoneally injected in the rats at time zero. At 5 h after, increased rectal temperature reached a plateau, and test compound was orally administrated in the rats. The anti-pyretic effect was evaluated at 2 h postdose of the test compound: the temperature at the time was compared to the temperature before LPS injection (at time zero), and the changes in temperature for 7 h were calculated. Data are expressed as the mean ± S.E.M. of 6–7 rats for each group (SPF/VAF, F344/DuCrj, male); $n = 6–7$.

[b] Oral inhibitory effect of COX-2 inhibitor **1** against edema formation by carrageenan on the paw of SPF/VAF male SD rats. Test compound was orally administrated in the rats at 1 h before intraplantar injection of carrageenan in the rats. At 3 h postinjection of carrageenan, inhibitory effect of the test compound against edema formation was evaluated: the foot volume at the time was compared to that of before carrageenan injection (at time zero), and the increases in volume for 3 h were calculated. Data are expressed as the mean ± S.E.M. of 6 rats for each group (SPF/VAF, Crj:CD(SD), male); $n = 6$.

[c] Oral inhibitory effect of COX-2 inhibitor **1** against prostaglandin E_2 production in carrageenan-stimulated foot of SPF/VAF male SD rats. Test compound was orally administrated in the rats at 1 h before intraplantar injection of carrageenan in the rats. The inhibitory effect of the test compound against prostaglandin E_2 production in the foot at 3 h after carrageenan injection was evaluated. Data are expressed as the mean ± S.E.M. of 6 rats for each group (SPF/VAF, Crj:CD(SD), male); $n = 6$.

[d] The evaluation studies of compounds **1–3** were independently performed. Control values for the evaluation studies of compound **1** were presented, respectively.

[e] ED_{50} value was calculated over a dose range of 0.3, 1.0, 3.0, and 10.0 mg/kg (p.o.) with linear-regression analysis plotted on a semilog scale. $r^2 = 0.9819$.

[f] ED_{40} value was calculated over a dose range of 0.3, 1.0, and 3.0 mg/kg (p.o.) with linear-regression analysis plotted on a semilog scale. $r^2 = 0.9933$.

[g] The results of compounds **2** and **3** were obtained from single dose study, respectively.

IC_{50} of compound **1** was 42.00 μM, compounds **2** and **3** showed less than 50% inhibition at a concentration of 100 μM on TXB_2 production, respectively. Consequently, these analogues are highly potent and selective COX-2 inhibitors *in vitro*. Especially, compound **1** demonstrated very attractive character, that is, the most potent COX-2 inhibitory activity among these analogues, with high selectivity for COX-2 inhibition over COX-1 inhibition. Thus, compound **1** showed (i) $IC_{50} = 0.00229$ μM against COX-2 activity in HUVEC assay and $IC_{50} = 3.618$ μM against COX-1 activity in HWP assay, hence 1580–fold COX-2-inhibition selectivity in the human cellular assays, and (ii) $IC_{50} = 0.331$ μM against COX-2 activity and $IC_{50} = 42.00$ μM against COX-1 activity in HWB assays, hence 127–fold COX-2-inhibition selectivity in the assays, respectively. On the basis of these encouraging results, these compounds were evaluated *in vivo* as the next step of this study.

3.2.2. In vivo oral activities in the rats

To address and identify an orally potent COX-2 inhibitor as an anti-pyretic agent *in vivo*, inhibitory activities against systemic-inflammatory body-temperature increase model stimulated by intraperitoneally injected-LPS in specific pathogen free and virus antibody free (SPF/VAF) male Fischer 344 (F344) rats *per os* (p.o.) were measured for compounds **1–3**. In this *in vivo* fever model, the increased temperature had reached a plateau at 5 h after LPS injection, and test compound was orally administrated at that time. The oral anti-pyretic effect for the compound was measured at 2 h postdose of the compound. The results were shown in Table 3 and Fig. 6.

Actually, compounds **1–3** displayed statistically significant oral anti-pyretic effects, that is, 51.88–78.17% inhibitions against LPS-stimulated fever in the rats at 10 mg/kg (p.o.), respectively. Notably, compound **1** demonstrated highly potent anti-pyretic activity in a dose-dependent manner over a dose concentration range of 0.3, 1.0, 3.0, and 10 mg/kg (p.o.), that is, 78.17% inhibition ($p < 0.001$) at 10 mg/kg and the calculated ED_{50} value was 1.68 mg/kg. The correlation between dose amount and %inhibition over the dose range was linear on a semilog plot ($r^2 = 0.9819$). Also, compound **2** showed 51.88% inhibitory activity ($p < 0.001$) and compound **3** showed 70.73% inhibitory activity ($p < 0.001$) at 10 mg/kg (p.o.), respectively. Hence, compound **1** displayed the most potent oral anti-pyretic efficacy among these compounds at 10 mg/kg (p.o.) in the fever model in the rats.

On the other hand, compound **1** was characterized for *in vivo* oral anti-inflammatory effect in peripheral-inflammation model in rats. Thus, to evaluate anti-inflammatory efficacy, oral inhibitory effect against edema-swelling stimulated by intraplantarly injected-carrageenan in the hind paw of SPF/VAF male Sprague–Dawley (SD) rats (p.o.) was measured for compound **1** [63–65]. Compound **1** was administrated at 1 h before carrageenan-injection and the swelling was measured before and at 3 h after carrageenan-injection. As a result, compound **1** showed statistically significant oral anti-edematous effect, that is, 45.68% inhibition ($p < 0.01$) at 3 mg/kg (p.o.) and the calculated ED_{40} value was 2.07 mg/kg over a dose range of 0.3, 1.0, and 3.0 mg/kg

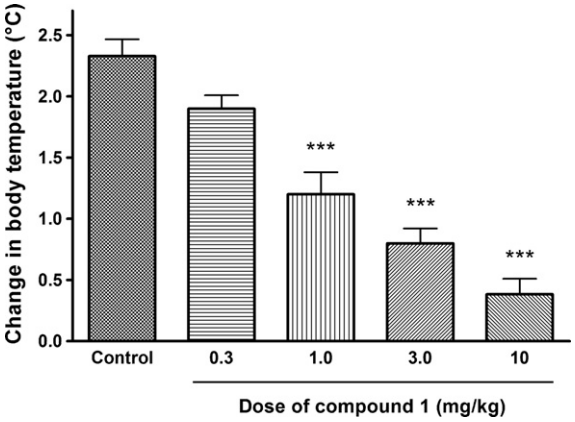

Fig. 6. Oral anti-pyretic effect of compound **1** against LPS-induced fever in SPF/VAF male F344 rats. LPS was intraperitoneally injected in the rats at time zero. At 5 h after, increased rectal temperature reached a plateau, and test compound was orally administrated in the rats. The temperature at 2 h postdose of the test compound was compared to the temperature before LPS injection (at time zero), and the changes in temperature for 7 h were calculated. *P*: One-way ANOVA followed by Dunnett's multiple comparison tests versus control; ***$p < 0.001$ significant difference from the control group; Data are expressed as the mean ± S.E.M. of 6 or 7 rats (SPF/VAF, F344/DuCrj, male); $n = 6–7$.

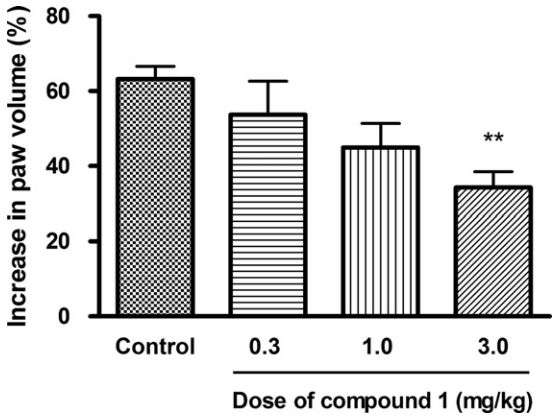

Fig. 7. Oral anti-inflammatory effect of compound **1** against carrageenan-induced edema formation on the paw of SPF/VAF male SD rats. Test compound was orally administrated in the rats at 1 h before intraplantar injection of carrageenan in the rats. By comparison of before (at time zero) and at 3 h after carrageenan injection, the increases in foot volume for 3 h were calculated. *P*: One-way ANOVA followed by Dunnett's multiple comparison tests versus control; $^{**}p < 0.01$ significant difference from the control group; Data are expressed as the mean ± S.E.M. of 6 rats (SPF/VAF, Crj:CD(SD), male); $n = 6$.

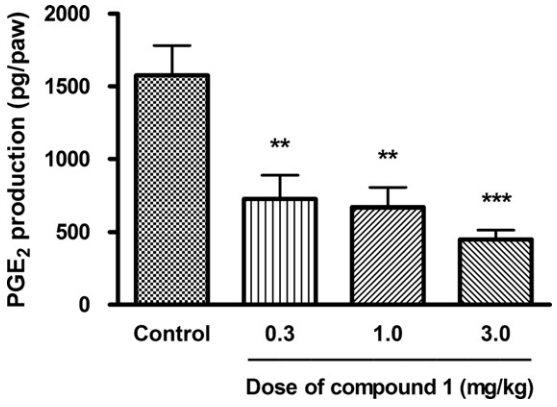

Fig. 8. Oral suppressive effect of compound **1** against prostaglandin E_2 production in carrageenan-stimulated foot of SPF/VAF male SD rats. Test compound was orally administrated in the rats at 1 h before intraplantar injection of carrageenan in the rats. Prostaglandin E_2 production in the foot at 3 h after carrageenan injection was evaluated. *P*: One-way ANOVA followed by Dunnett's multiple comparison tests versus control; $^{**}p < 0.01$, $^{***}p < 0.001$ significant difference from the control group. Data are expressed as the mean ± S.E.M. of 6 rats (SPF/VAF, Crj:CD(SD), male); $n = 6$.

(p.o.) as shown in Table 3 and Fig. 7. As well, oral suppressive effect against PGE_2 production stimulated by carrageenan in the SD rat foot, that was the edema-formation site in the above peripheral-inflammation model, was measured for compound **1** [66]. Indeed, compound **1** showed statistically significant oral inhibitory activity against PGE_2 production in the foot, that is, 88.16% inhibition ($p < 0.01$) at 3 mg/kg (p.o.) as shown in Table 3 and Fig. 8.

Table 4
Physicochemical properties of COX-2 inhibitors **1**–**3**.

Compounds	Physicochemical properties				
	Size	TPSA	Lipophilicity	HBD[a]	HBA[b]
	MW	Å^2	ACD log $D_{7.4}$[c]	Number	Number
1	376.33	83.05	−0.96	2	4
2	388.34	83.05	−0.90	2	4
3	354.79	83.05	−0.83	2	4

[a] HBD, hydrogen bond donor.
[b] HBA, hydrogen bond acceptor.
[c] Predicted by ACD/Laboratories 9.0.

3.2.3. Physicochemical properties

It is noteworthy that physicochemical properties of novel designed compounds **1–3** show acceptability for *in vivo* oral activities as shown in Table 4. Thus, the properties in terms of significant factors for oral activities of general marketable drugs in clinical and potential drugs *in vivo* [74–76,77a,77b] are actually appropriate for orally potent inhibitory activities in the pyresis model in rats for compounds **1–3** and in the edema-formation model in rats for compound **1** in the present study. For example, as the physicochemical properties for compounds **1–3**, molecular weight (MW) values are lower than 400, topological polar surface area (TPSA) values are 83.05 Å^2, and lipophilicity values calculated as ACD log D at pH 7.4 are −0.96 to −0.83, respectively. Furthermore, in common with the respective structure of compounds **1–3**, the numbers of hydrogen bond donor (HBD) are two and the numbers of hydrogen bond acceptor (HBA) are four, that is, one carboxyl group as one HBD functionality and two HBA functionalities, one secondary-amino group of indole ring as one HBD functionality whereas this aromatic and neutral potion has no HBA functionality, one carbonyl group as one HBA functionality, and one pyridinyl group as one HBA functionality, respectively.

On the other hand, as the structural features for the compounds described above, the low (or less than certain level) lipophilicities under physiological plasma condition with the multisite hydrophilic functionalities (for example, HBD functionalities at plural sites) are preferable for preventing their passive diffusion across blood–brain barrier (BBB) while still retaining other favorable properties of the compounds with systemic administration [77c]. Actually, several certain {2-[(2-aryl)carbonyl]-(6- or 5-substituted)-1*H*-indol-3-yl}acetic acid analogues, that have similar physicochemical properties such as lipophilicity and size, and have similar structural features such as the same multisite HBD functionalities (for hydrophilic functionalities) as that of compounds **1–3**, indicated high plasma-to-brain selectivity in SD rats *per os*, thus, their plasma/brain ratios = 23.8 to 55.4 (10 mg/kg, 1 h, p.o.) [that is, plasma levels (μg/mL)/brain levels (μg/mg) = 5.96/0.250 to 7.76/0.140; further data not shown]. Therefore, compounds **1–3** would have higher exposure levels in the plasma than in the brain *per os*, as well.

Taken together, these physicochemical and structural characters for compounds **1–3**, together with their potent intrinsic COX-2 inhibitory activities, would lead to orally potent efficacies in the present fever and edema-swelling models *in vivo*. These unique features for compounds **1–3** were also discussed later in viewpoints of druglikeness and site of actions (see Section 4).

4. Discussion

As significant findings of the present drug-discovery study, novel designed acid-type compounds **1–3** showed potent and highly selective *in vitro* COX-2 inhibitory activities in human cellular assays and in HWB assays, and demonstrated orally potent *in vivo* anti-pyretic activities in the systemic-inflammatory fever model by intraperitoneally injected-LPS in the F344 rats. Significantly, for compound **1**, the most potent *in vivo* oral anti-pyretic efficacy among these compounds at 10 mg/kg (p.o.) in the fever model in rats was in line with the most potent *in vitro* inhibitory activities against COX-2 actions among these compounds in the COX-2-induced human cellular and whole-blood assays. Also, compound **1** displayed orally potent *in vivo* anti-inflammatory efficacy with suppression of PGE_2 production in the peripheral-inflammatory edema-formation model by intraplantarly injected-carrageenan in the SD rats.

As mentioned before, following inflammatory or tissue-injury stimuli/signals, COX-2 is induced in the peripheral tissues such as

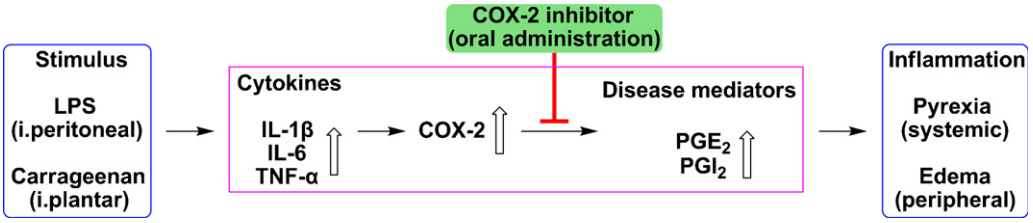

Fig. 9. The mechanisms of orally potent anti-pyretic effect in the LPS-induced fever model and anti-edematous effect in the carrageenan-induced edema-formation model for COX-2 inhibitor.

macrophages, monocytes, synoviocytes, blood, liver, and lung, as well as in the nerve systems such as peripheral nerves, spinal cord or brain. And then, COX-2 action-derived inflammatory-signals such as PGs are released, thereby causing pyrexia and edema as systemic- and/or peripheral-inflammatory symptoms. For example, systemic fever occurs owing to bacterial infection via the stimulation of extracellular endotoxic bacterial products such as LPS. As well, carrageenan injection is well known as a procedure to form peripheral-inflammatory edema *in vivo*. And COX-2 plays crucial key roles in these pathophysiological events (Fig. 9 illustrates the mechanisms of orally potent efficacies of an intrinsically potent COX-2 inhibitor with appropriate property to suppress the events *in vivo*).

Thus, it has been studied in detail for time-dependent multiphasic mechanisms of systemic fever development following peripheral endotoxic stimulation [12–15]. In the case of endotoxic LPS stimulation, at the first phase, the endotoxic peripheral stimuli triggers IL-1β and TNF-α releases that induce COX-2 expression in the macrophages (in peritonea and other sites), monocytes, blood, endothelial cells, liver, and lung; then COX-2 produces PGH_2, followed by catabolism of PGH_2 with PGE synthases (PGESs) to form the febrile mediator PGE_2 [1,3,5,7,78]. In succession, PGE_2 that is released from the tissues or sites is transported across blood–brain barrier (BBB) into brain [12–15,79,80], and binds to EP_1 or EP_3 receptor that induces increased body temperature [10,81–83]. It is reported as well that fever by intraperitoneally injected LPS was blocked in COX-2 knockout mice, but not in COX-1 knockout mice [16]. On the other hand, IL-1β- or LPS-induced COX-2 action for PGE_2 production was strongly inhibited by compounds **1**–**3** as shown in the present *in vitro* studies. Therefore, it is reasonable that the oral anti-pyretic efficacies of compounds **1**–**3** in this study are derived from their potent intrinsic suppressive-effects on COX-2-dependent PGE_2 production in the peripheral sites.

Also, it has been described in detail that mechanisms of peripheral-inflammatory edema-formation (and peripheral-inflammatory pain) by carrageenan comprise time-dependent multi phases. Thus, it is reported that carrageenan induces IL-6 and TNF-α releases locally [84], and the expression/upregulation of COX-2 in the peripheral carrageenan-injected site causes production of inflammatory mediators PGE_2 and PGI_2 with PGESs and PGI_2 synthase (PGIS), respectively, thereby leading to inflammatory edema-formation (and hypersensitivity) at the site via the activation of EP and IP receptors by PGE_2 and PGI_2, respectively [1,5,7,10,85–87]. In the present *in vitro* study, COX-2-derived production of PGE_2 and of 6-keto-$PGF_{1\alpha}$, that is degraded stable form of PGI_2, was strongly inhibited by compound **1** (as well as compounds **2** and **3**), respectively. Hence, it is also reasonable that the oral anti-edematous efficacy of compound **1** in this study is due to its intrinsic inhibitory activities against the release of COX-2-derived inflammatory mediators PGE_2 and PGI_2 in the peripheral site, which is in line with the reported studies of COX-2-dependent edema-formation mechanisms.

Moreover, with regard to a viewpoint of similarity to other COX inhibitors, compounds **1**–**3** are novel acid-type compounds whose physicochemical properties are appropriate for the orally potent *in vivo* efficacies as mentioned, and actually, these compounds effectively worked as an orally potent anti-pyretic agent, respectively, in the systemic-inflammatory fever model in rats. Also, compounds **1**–**3** are estimated to have peripheral selectivity by their physicochemical properties and structural characteristics such as very low lipophilicity under physiological pH condition and multisite hydrogen-bonding functionalities. Indeed, compound **1** had oral inhibitory efficacies against inflammatory swelling and PGE_2 production in the peripheral-inflammation model in rats. Consequently, the site of actions for these compounds in these *in vivo* studies would be associated with their potent intrinsic COX-2 inhibitory activities at peripheral sites after oral administration. As described, both the mechanisms of inflammatory febrile-response pathways from peripheral to brain and the mechanisms of inflammatory edema-formation in the peripheral are estimated for the compound(s) in the present study, and are accordance with reported studies. Besides, the intrinsic inhibitory effects for the compounds in the CNS against COX-2-related inflammatory signal pathways such as PG synthesis in the spinal cord is possibly contributed to the present anti-inflammatory effects as reported by other study groups [8,22,36,88].

Taken together, the present novel COX-2 inhibitors **1**–**3** with unique acid-type structure might be very useful as potential drugs to discover and develop an orally potent new-class of COX-2 inhibitor for the clinical treatment of pyrexia, inflammation, and pain. Further characterization of the compound might be also helpful for the treatment of other inflammatory diseases such as RA, OA or cancers related to chronic inflammation, as well as vascular endothelial function in coronary artery disease, and LPS-induced cardiovascular failure or liver injury. As well, assessment of COX-2 inhibitor for safety index of potential cardiovascular risk in long-term use would be important as mentioned already. Moreover, these compounds might be effective as unique tools to elucidate further functional, physiological, and pharmacological studies associated with the mechanisms of COX-2-involving pathways including COX-2-dependent PG cascades.

5. Conclusions

In conclusion, novel designed [2-{[(4-substituted)-pyridin-2-yl]carbonyl}-(6- or 5-substituted)-1*H*-indol-3-yl]acetic acids **1**–**3** demonstrate potent and highly selective *in vitro* COX-2 inhibitions, and demonstrate orally potent *in vivo* anti-pyretic effects in systemic-inflammatory fever model by LPS in the F344 rats, that is, COX-2 inhibitors **1**–**3** are potential new-class anti-pyretic drugs. As well, compound **1** demonstrates orally potent *in vivo* anti-inflammatory effect against peripheral edema-formation model by carrageenan in the SD rats with suppression of PGE_2 production in the edema site, that is, compound **1** is a potential new-class anti-inflammatory drug. The significant findings of the unique acid-type COX-2 inhibitors might be also helpful for further drug discovery and development studies in terms of the clinical treatments of various inflammatory diseases such as pyrexia,

inflammation, and pain, also OA, RA or cancers related to chronic inflammation, as well as coronary artery disease and endotoxin-induced cardiovascular- or liver-disease. Furthermore, these compounds might be useful tools for further physiological and pharmacological investigations involved in COX-2 pathways including COX-2-dependent PG cascades.

References

[1] Review: Funk CD. Prostaglandins and leukotrienes: advances in eicosanoid biology. Science 2001;294:1871–5.
[2] Funk CD, Funk LB, Kennedy ME, Pong AS, Fitzgerald GA. Human platelet/erythroleukemia cell prostaglandin G/H synthase: cDNA cloning, expression, and gene chromosomal assignment. FASEB J 1991;5:2304–12.
[3] Patrignani P, Panara MR, Greco A, Fusco O, Natoli C, Iacobelli S, et al. Biochemical and pharmacological characterization of the cyclooxygenase activity of human blood prostaglandin endoperoxide synthases. J Pharmacol Exp Ther 1994;271:1705–12.
[4] Smith WL, Garavito RM, DeWitt DL. Prostaglandin endoperoxide H synthase (cyclooxygenase)-1 and -2. J Biol Chem 1996;271:33157–60.
[5] Review: Simmons DL, Botting RM, Hla T. Cyclooxygenase isozymes: the biology of prostaglandin synthesis and inhibition. Pharmacol Rev 2004;56:387–437.
[6] Malkowski MG, Ginell SL, Smith WL, Garavito RM. The productive conformation of arachidonic acid bound to prostaglandin synthase. Science 2000;289:1933–7.
[7] Zeilhofer HU. Prostanoids in nociception and pain. Biochem Pharmacol 2007;73:165–74.
[8] Review: Vanegas H, Schaible H-G. Prostaglandins and cyclooxygenases in the spinal cord. Prog Neurobiol 2001;64:327–63.
[9] Review: Kojima F, Kapoor M, Kawai S, Crofford LJ. New insights into eicosanoid biosynthetic pathways: implication for arthritis. Expert Rev Clin Immunol 2006;2:277–91.
[10] Sugimoto Y, Narumiya S, Ichikawa A. Distribution and function of prostanoid receptors: studies from knockout mice. Prog Lipid Res 2000;39:289–314.
[11] Kang RY, Freire-Moar J, Sigal E, Chu C-Q. Expression of cyclooxygenase-2 in human and an animal model of rheumatoid arthritis. Br J Rheumatol 1996;35:711–8.
[12] Review: Blatteis CM. Endotoxic fever: new concepts of its regulation suggest new approaches to its management. Pharmacol Ther 2006;111:194–223.
[13] Ivanov AI, Pero RS, Scheck AC, Romanovsky AA. Prostaglandin E_2-synthesizing enzymes in fever: differential transcriptional regulation. Am J Physiol Regul Integr Comp Physiol 2002;283:R1104–17.
[14] Romanovsky AA, Almeida MC, Aronoff DM, Ivanov AI, Konsman JP, Steiner AA, et al. Fever and hypothermia in systemic inflammation: recent discoveries and revisions. Front Biosci 2005;10:2193–216.
[15] Steiner AA, Ivanov AI, Serrats J, Hosokawa H, Phayre AN, Robbins JR, et al. Cellular and molecular bases of the initiation of fever. PLoS Biol 2006;4:1517–24.
[16] Li S, Wang Y, Matsumura K, Ballou LR, Morham SG, Blatteis CM. The febrile response to lipopolysaccharide is blocked in cyclooxygenase-$2^{-/-}$, but not in cyclooxygenase-$1^{-/-}$ mice. Brain Res 1999;825:86–94.
[17] Review: Vane JR, Botting RM. The mechanism of action of aspirin. Thromb Res 2003;110:255–8.
[18] Review: Burian M, Geisslinger G. COX-dependent mechanisms involved in the antinociceptive action of NSAIDs at central and peripheral sites. Pharmacol Ther 2005;107:139–54.
[19] Laine L. GI risk and risk factors of NSAIDs. J Cardiovasc Pharmacol 2006;47(Suppl. 1):S60–6.
[20] Radi ZA, Khan NK. Effects of cyclooxygenase inhibition on the gastrointestinal tract. Exp Toxicol Pathol 2006;58:163–73.
[21] Warner TD, Giuliano F, Vojnovic I, Bukasa A, Mitchell JA, Vane JR. Nonsteroid drug selectivities for cyclo-oxygenase-1 rather than cyclo-oxygenase-2 are associated with human gastrointestinal toxicity: a full in vitro analysis. Proc Natl Acad Sci USA 1999;96:7563–8.
[22] Yaksh TL, Dirig DM, Conway CM, Svensson C, Luo ZD, Isakson PC. The acute antihyperalgesic action of nonsteroidal, anti-inflammatory drugs and release of spinal prostaglandin E_2 is mediated by the inhibition of constitutive spinal cyclooxygenase-2 (COX-2) but not COX-1. J Neurosci 2001;21:5847–53.
[23] Beiche F, Scheuerer S, Brune K, Geisslinger G, Goppelt-Struebe M. Up-regulation of cyclooxygenase-2 mRNA in the rat spinal cord following peripheral inflammation. FEBS Lett 1996;390:165–9.
[24] O'Neill GP, Ford-Hutchinson AW. Expression of mRNA for cyclooxygenase-1 and cyclooxygenase-2 in human tissues. FEBS Lett 1993;330:156–60.
[25] Hampel SL, Monick MM, Huninghake GW. Lipopolysaccharide induces prostaglandin H synthase-2 protein and mRNA in human alveolar macrophages and blood monocytes. J Clin Invest 1994;93:391–6.
[26] Review: Steer SA, Corbett JA. The role and regulation of COX-2 during viral infection. Viral Immunol 2003;16:447–60.
[27] Bazan NG. COX-2 as a multifunctional neuronal modulator. Nat Med 2001;7:414–5.
[28] Hla T, Neilson K. Human cyclooxygenase-2 cDNA. Proc Natl Acad Sci USA 1992;89:7384–8.
[29] Review: Bishop-Bailey D, Hla T, Mitchell JA. Cyclo-oxygenase-2 in vascular smooth muscle. Int J Mol Med 1999;3:41–8.
[30] Siegle I, Klein T, Backman JT, Saal JG, Nüsing RM, Fritz P. Expression of cyclooxygenase 1 and cyclooxygenase 2 in human synovial tissue. Differential elevation of cyclooxygenase 2 in inflammatory joint diseases. Arthritis Rheum 1998;41:122–9.
[31] Stamp LK, Cleland LG, James MJ. Upregulation of synoviocyte COX-2 through interactions with T lymphocytes: role of interleukin 17 and tumor necrosis factor-α. J Rheumatol 2004;31:1246–54.
[32] Amin AR, Attur M, Patel RN, Thakker GD, Marshall PJ, Rediske J, et al. Super induction of cyclooxygenase-2 activity in human osteoarthritis-affected cartilage. Influence of nitric oxide. J Clin Invest 1997;99:1231–7.
[33] Geng Y, Blanco FJ, Cornelisson M, Lotz M. Regulation of cyclooxygenase-2 expression in normal human articular chondrocytes. J Immunol 1995;155:796–801.
[34] Pouliot M, Gilbert C, Borgeat P, Borgeat P, Poubelle PE, Bourgoin S, et al. Expression and activity of prostaglandin endoperoxide synthase-2 in agonist-activated human neutrophils. FASEB J 1998;12:1109–23.
[35] Hu W, Mathey E, Hartung H-P, Kieseier BC. Cyclo-oxygenases and prostaglandins in acute inflammatory demyelination of the peripheral nerve. Neurology 2003;61:1774–9.
[36] Hay C, de Belleroche J. Carrageenan-induced hyperalgesia is associated with increased cyclo-oxygenase-2 expression in spinal cord. NeuroReport 1997;8:1249–51.
[37] For example: Wu KK. Differential cyclooxygenase-2 transcriptional control in proliferating versus quiescent fibroblasts. Prostaglandins Other Lipid Mediat 2007;83:175–81.
[38] For example: Coffey RJ, Hawkey CJ, Damstrup L, Graves-Deal R, Daniel VC, Dempsey PJ, et al. Epidermal growth factor receptor activation induces nuclear targeting of cyclooxygenase-2, basolateral release of prostaglandins, and mitogenesis in polarizing colon cancer cells. Proc Natl Acad Sci USA 1997;94:657–62.
[39] Duque J, Díaz-Muñoz MD, Fresno M, Iñiguez MA. Up-regulation of cyclooxygenase-2 by interleukin-1β in colon carcinoma cells. Cell Signal 2006;18:1262–9.
[40] Khan AA, Iadarola M, Yang H-YT, Dionne RA. Expression of COX-1 and COX-2 in a clinical model of acute inflammation. J Pain 2007;8:349–54.
[41] Review: Mitchell JA, Warner TD. Cyclo-oxygenase-2: Pharmacology, physiology, biochemistry and relevance to NSAID therapy. Br J Pharmacol 1999;128:1121–32.
[42] Dormond O, Foletti A, Paroz C, Rüegg C. NSAIDs inhibit αVβ3 integrin-mediated and Cdc42/Rac-dependent endothelial-cell spreading, migration and angiogenesis. Nat Med 2001;7:1041–7.
[43] Zhao Q-T, Yue S-Q, Cui Z, Wang Q, Cui X, Zhai H-H, et al. Potential involvement of the cyclooxygenase-2 pathway in hepatocellular carcinoma-associated angiogenesis. Life Sci 2007;80:484–92.
[44] Iwata C, Kano MR, Komuro A, Oka M, Kiyono K, Johansson E, et al. Inhibition of cyclooxygenase-2 suppresses lymph node metastasis via reduction of lymphangiogenesis. Cancer Res 2007;67:10181–9.
[45] Hull MA, Faluyi OO, Ko CWS, Holwell S, Scott DJ, Cuthbert RJ, et al. Regulation of stromal cell cycloocygenase-2 in the $Apc^{Min/+}$ mouse model of intestinal tumorigenesis. Carcinogenesis 2006;27:382–91.
[46] Chen J-H, Wu C-W, Kao H-L, Chang H-M, Li AL-Y, Liu T-Y, et al. Effects of COX-2 inhibitor on growth of human gastric cancer cells and its relation to hepatocyte growth factor. Cancer Lett 2006;239:263–70.
[47] Reddy BS, Rao CV. Novel approaches for colon cancer prevention by cyclooxygenase-2 inhibitors. J Environ Pathol Toxicol Oncol 2002;21:155–64.
[48] Krysan K, Reckamp KL, Sharma S, Dubinett SM. The potential and rationale for COX-2 inhibitors in lung cancer. Anti-Cancer Agents Med Chem 2006;6:209–20.
[49] Chenevard R, Hürlimann D, Béchir M, Enseleit F, Spieker L, Hermann M, et al. Selective COX-2 inhibition improves endothelial function in coronary artery disease. Circ J Am Heart Assoc 2003;107:405–9.
[50] Höcherl K, Dreher F, Kurtz A, Bucher M. Cyclooxygenase-2 inhibition attenuates lipopolysaccharide-induced cardiovascular failure. Hypertens J Am Heart Assoc 2002;40:947–53.
[51] Oitate M, Hirota T, Murai T, Miura S, Ikeda T. Covalent binding of rofecoxib, but not other cyclooxygenase-2 inhibitors, to allysine aldehyde in elastin of human arota. Drug Metab Dispos 2007;35:1846–52.
[52] Hinz B, Renner B, Brune K. Drug insight: cyclo-oxygenase-2 inhibitors—a critical appraisal. Nat Clin Pract Rhum 2007;3:552–60.
[53] Kowalski ML, Makowska J. Use of nonsteroidal anti-inflammatory drugs in patients with aspirin hypersensivity. Safety of cyclo-oxygenase-2 inhibitors. Treat Respir Med 2006;5:399–406.
[54] Staats PS. Pain management and beyond: evolving concepts and treatments involving cyclooxygenase inhibition. J Pain Symptom Manage 2002;24(1S):S4–9.
[55] Case FH, Kasper TJ. The preparation of some substituted 2,6-bis-(2-pyridyl)-pyridines. J Am Chem Soc 1956;78:5842–4.
[56] Constable EC, Heirtzler F, Neuburger M, Zehnder M. Steric control of directional isomerism in dicopper(I) helicates of asymmetrically substituted 2,2′:6′,2″:2″,6‴-quaterpyridine derivatives. J Am Chem Soc 1997;119:5606–17.
[57] Carling RW, Leeson PD, Moore KW, Smith JD, Moyes CR, Mawer IM, et al. 3-Nitro-3,4-dihydro-2(1H)-quinolones. Excitatory amino acid antagonists acting at glycine-site NMDA and (RS)- α-amino-3-hydroxy-5-methyl-4-isoxazolepropionic acid receptors. J Med Chem 1993;36:3397–408.
[58] Riendeau D, Percival MD, Boyce S, Brideau C, Charleson S, Cromlish W, et al. Biochemical and pharmacological profile of a tetrasubstituted furanone as a highly selective COX-2 inhibitor. Br J Pharmacol 1997;121:105–17.

[59] Moore PF, Larson DL, Otterness IG, Weissman A, Kadin SB, Sweeney FJ, et al. Tenidap, a structurally novel drug for the treatment of arthritis: antiinflammatory and analgesic properties. Inflamm Res 1996;45:54–61.
[60] Brideau C, Kargman S, Liu S, Dallob AL, Ehrich EW, Rodger IW, et al. A human whole blood assays for clinical evaluation of biochemical efficacy of cyclooxygenase inhibitors. Inflamm Res 1996;45:68–74.
[61] Young JM, Panah S, Satchawatcharaphong C, Cheung PS. Human whole blood assays for inhibition of prostaglandin G/H synthase-1 and -2 using A23187 and lipopolysaccharide stimulation of thromboxane B_2 production. Inflamm Res 1996;45:246–53.
[62] Glaser K, Sung M-L, O'Neill K, Belfast M, Hartman D, Carlson R, et al. Etodolac selectively inhibits human prostaglandin G/H synthase 2 (PGHS-2) versus human PGHS-1. Eur J Pharmacol 1995;281:107–11.
[63] Winter CA, Risley EA, Nuss GV. Carrageenin-induced edema in hind paw of the rat as an assay for antiiflammatory drugs. Proc Soc Exp Biol Med 1962;111:544–7.
[64] Lombardino JG, Otterness IG, Wiseman EH. Acidic anti-inflammatory agents-correlations of some physical, pharmacological and clinical data. Arzneimittle Forschung 1975;25:1629–35.
[65] Gracia Leme J, Hamamura L, Leite MP, Rocha e Silva M. Pharmacological analysis of the acute inflammatory process induced in the rat's paw by local injection of carrageenin and by heating. Br J Pharmacol 1973;48:88–96.
[66] Opas EE, Dallob A, Herold E, Luell S, Humes JL. Pharmacological modulation of eicosanoid levels and hyperalgesia in yeast-induced inflammation. Biochem Pharmacol 1987;36:547–51.
[67] Patel BA, Ziegler CB, Cortese NA, Plevyak JE, Zebovitz TC, Terpko M, et al. Palladium-catalyzed vinylic substitution reactions with carboxylic acid derivatives. J Org Chem 1977;42:3903–7.
[68] Knowles JP, Whiting A. The Heck–Mizoroki cross-coupling reaction: a mechanistic perspective. Org Biomol Chem 2007;5:31–44.
[69] Garcia Ruano JL, Pedregal C, Rodriguez JH. Synthesis and conformational analysis of some oxisuran metabolites and their O-methylderivatives. Tetrahedron 1987;43:4407–16.
[70] Eisch JJ, Gopal H, Russo DA. Preparation and aluminum chloride induced rearrangement of cyclopropylpyridines. J Org Chem 1974;39:3110–4.
[71] Shuman RT, Ornstein PL, Paschal JW, Gesellchen PD. An improved synthesis of homoproline and derivatives. J Org Chem 1990;55:738–41.
[72] Olszanecki R, Gębska A, Korbut R. Production of prostacyclin and prostaglandin E_2 in resting and IL-1β-stimulated A459. HUVEC and hybrid EA. HY 926 cells. J Physiol Pharmacol 2006;57:649–60.
[73] James MJ, Penglis PS, Caughey GE, Demasi M, Cleland LG. Eicosanoid production by human monocytes: does COX-2 contribute to a self-limiting inflammatory response? Inflamm Res 2001;50:249–53.
[74] Lipinski CA, Lombardo F, Dominy BW, Feeney PJ. Experimental and computational approaches to estimate solubility and permeability in drug discovery and development settings. Adv Drug Deliv Rev 1997;23:3–25.
[75] Kelder J, Grootenhuis PDJ, Bayada DM, Delbressine LPC, Ploemen J-P. Polar molecular surface as a dominating determinant for oral absorption and brain penetration of drugs. Pharm Res 1999;16:1514–9.
[76] Ertl P, Rohde B, Selzer P. Fast calculation of molecular polar surface area as a sum of fragment-based contributions and its application to the prediction of drug transport properties. J Med Chem 2000;43:3714–7.
[77] The details of distinct drug-design and SAR studies of novel NOP receptor agonist as orally potent anxiolytic and of novel NOP receptor agonist as systemically potent analgesic mentioned in the present article were including in the following (Hayashi et al.), that is, Refs [77a, 77b] and Ref [77c], respectively:;
(a) Hayashi S, Hirao A, Imai A, Nakamura H, Murata Y, Ohashi K, et al. Novel non-peptide nociceptin/orphanin FQ receptor agonist, 1-[1-(1-methylcyclooctyl)-4-piperidinyl]-2-[(3R)-3-piperidinyl]-1H-benzimidazole: design, synthesis, and structure–activity relationship of oral receptor occupancy in the brain for orally potent antianxiety drug. J Med Chem 2009;52:610–25;
(b) Hayashi S, Hirao A, Nakamura H, Yamamura K, Mizuno K, Yamashita H. Discovery of 1-[1-(1-methylcyclooctyl)-4-piperidinyl]-2-[(3R)-3-piperidinyl]-1H-benzimidazole: integrated drug-design and structure–activity relationships for orally potent, metabolically stable, and potential-risk reduced novel non-peptide nociceptin/orphanin FQ receptor agonist as antianxiety drug. Chem Biol Drug Des 2009;74:369–81;
(c) Hayashi S, Nakata E, Morita A, Mizuno K, Yamamura K, Kato A, et al. Discovery of {1-[4-(2-{hexahydropyrrolo[3,4-c]pyrrol-2(1H)-yl}-1H-benzimidazol-1-yl)piperidin-1-yl]cyclooctyl}methanol, systemically potent novel non-peptide agonist of nociceptin/orphanin FQ receptor as analgesic for the treatment of neuropathic pain: design, synthesis, and structure–activity relationships. Bioorg Med Chem 2010;18:7675–99
[78] Deforge LE, Kenney JS, Jones ML, Warren JS, Remick DG. Biphasic production of IL-8 in lipopolysaccharide (LPS)-stimulated human whole blood. Separation of LPS- and cytokine-stimulated components using anti-tumor necrosis factor and anti-IL-1 antibodies. J Immunol 1992;148:2133–41.
[79] Kis B, Isse T, Snipes JA, Chen L, Yamashita H, Ueta Y, Busija DW. Effects of LPS stimulation on the expression of prostaglandin carriers in the cells of the blood–brain and blood–cerebrospinal fluid barriers. J Appl Physiol 2006;100:1392–9.
[80] Engblom D, Ek M, Saha S, Ericsson-Dahlstrand A, Jakobbson P-J, Blomqvist A. Prostaglandins as inflammatory messengers across the blood–brain barrier. J Mol Med 2002;80:5–15.
[81] Oka T, Oka K, Saper CB. Contrasting effects of E type of prostaglandin (EP) receptor agonists on core body temperature in rats. Brain Res 2003;968:256–62.
[82] Ivanov AI, Scheck AC, Romanovsky AA. Expression of genes controlling transport and catabolism of prostaglandin E_2 in lipopolysaccaride fever. Am J Physiol Regul Integr Comp Physiol 2003;284:R698–706.
[83] Ushikubi F, Segi E, Sugimoto Y, Murata T, Matsuoka T, Kobayashi T, et al. Impaired febrile response in mice lacking the prostaglandin E receptor subtype EP_3. Nature 1998;395:281–4.
[84] Romano M, Faggioni R, Sironi M, Sacco S, Echtenacher B, Di Santo E, et al. Carrageenan-induced acute inflammation in the mouse air pouch synovial model. Role of tumour necrosis factor. Mediat Inflamm 1997;6:32–8.
[85] Padi SSV, Jain NK, Singh S, Kulkarni SK. Pharmacological profile of paracoxib: a novel, potent injectable selective cyclooxygenase-2 inhibitor. Eur J Pharmacol 2004;491:69–76.
[86] Posadas I, Bucci M, Roviezzo F, Rossi A, Parente L, Sautebin L, et al. Carrageenan-induced mouse paw oedema is biphasic, age-weight dependent and displays differential nitric oxide cyclooxygenase-2 expression. Br J Pharmacol 2004;142:331–8.
[87] Claudino RF, Kassuya CAL, Ferreira J, Calixto JB. Pharmacological and molecular characterization of the mechanisms involved in prostaglandin E_2-induced mouse paw edema. J Pharmacol Exp Ther 2006;318:611–8.
[88] Svensson CI, Yaksh TL. The spinal phospholipase–cyclooxygenase–prostanoid cascade in nociceptive processing. Ann Rev Pharmacol Toxicol 2002;42:553–83.